Paper by HHoextra

Abstract: The paper presents a direct, i.e. non-recursive, way on the basis of analytical expressions to compute the number of ways one may walk on the surface of a Bucky-ball between two arbitrarily chosen (out of 60) vertex points of the ball, in a given number of steps along the sides of hexagons and pentagons. In addition, the approach may provide easy to evaluate formulae giving the number of visits to intermediate vertex points during such a trip. The presented theory is based on the so-called tight binding model utilizing group theory, with the latter using only a small part of the symmetry properties of the Bucky-ball. The full theory is presented as well as a number of results of computations therewith. Possible fields of applications are mentioned and discussed in short.

Copyright

Author paper: HJWM Hoekstra
Title Paper: *Walking on a Bucky ball*

Published in-house via http://hhoextra.nl/Considerations

Walking on a Bucky Ball

Abstract: The paper presents a direct, i.e. non-recursive, way on the basis of analytical expressions to compute the number of ways one may walk on the surface of a Bucky-ball between two arbitrarily chosen (out of 60) vertex points of the ball, in a given number of steps along the sides of hexagons and pentagons. In addition, the approach may provide easy to evaluate formulae giving the number of visits to intermediate vertex points during such a trip. The presented theory is based on the so-called tight binding model utilizing group theory, with the latter using only a small part of the symmetry properties of the Bucky-ball. The full theory is presented as well as a number of results of computations therewith. Possible fields of applications are mentioned and discussed in short.

I. Introduction

Imagine: you and may be a few other creatures are living on a great Bucky ball (BB, see fig. 1) and you can move only along the edges of the pentagons and hexagons stepping from adjacent vertex point to adjacent vertex point. The same holds for the other creatures which could be friends, the person of your dreams, migrating animals, but also dictators and other criminals. You may have a lot of questions about the number of ways you can reach some other site or vertex point, or about the spreading of migrating animals (assuming a random walk) or many other related topics. It may also be desirable to know along which sites you may reach some other site, assuming a given number of steps. If you are in such situation or if you are curious to read more about the above and related things you may want to study this paper.

To indicate in formulae the position of a person or particle (or a localized function) on the BB it is convenient to use the simple bra-ket notation with, for example, a ket $|n\rangle$ indicating that its position is site n. The advantage of this notation – which is quite common in quantum mechanics – is that an inner product can easily be formulated via a bra, written like $\langle l|$, with $\langle l|m\rangle = \delta_{lm}$ (δ_{lm} is the Kronecker delta function, with $\delta_{lm} = 0$ if $l \neq m$ and $\delta_{ll} = 1, \forall l$). And, as we will see, in sect. II, it enables a simple expression for the step operators, transferring the particle from one site to other sites. But, instead of working with localized functions – representing the presence of you, a particle or some function localized on a certain site – we have chosen to tackle the topic in terms of a holistic, wave-mechanical approach. So, we will consider delocalized states corresponding to, for example, you or the particle being spread out over (part of) the BB. Their number will be 60 – owing to the number of sites on a BB and so the number of (localized) site functions – and each such spread-out state can be written as the sum of (also 60) localized states and vice versa. It turns out to be convenient to choose mentioned spread-out states as eigenfunctions of an operator (denoted here by $\mathcal{H}$) representing the transfer of each such a site state to its three neighbours. This approach opens the way to derive analytical expressions for the number of ways (NoWs) to travel between two given sites in a given number of steps and also to expressions for the number of visits (NoVs) to one or more intermediate sites while travelling this way.

The considered BB is quite well known and needs hardly any further introduction here, apart – may be – from the following. To refresh the memory we refer to figure 1 and mention that the BB consists of 20 hexagons, 12 pentagons (i.e., the number of faces, $F = 32$), ($V =$) 60 vertices and ($E =$) 90 edges, satisfying Euler-Descartes theorem: $F+V = E+2$. The approach for the derivation of NoWs and NoVs will be based on the so-called tight binding model (TBM), in which it is assumed that (one may think of e.g. electronic) energy levels arise from the interaction between neighbouring atoms or molecules. The TBM is also quite suitable owing to

its transparent terminology. In presented model the 60 vertices all support a single state (which is localized on the corresponding site in the absence of assumed TB interaction). Use will be made of Group Theory (GT) employing the five-fold symmetry of considered structure, enabling a considerable reduction of the computational time needed to numerically solve the eigenvalue equations – compared to solving the full problem with 60 basis functions. In addition the numerical inaccuracy will likely decrease. Using the full symmetry of the icosahedral group (which uses the full symmetry of the BB) could lead to a further lowering of the dimensionality of the matrices involved, but also may be more bookkeeping and a further lowering of the computation time – which is quite acceptable with the here presented approach using only five-fold symmetry – is not urgently required.

The motivation for presented research is in the first place curiosity but also the hope that someway it will lead to something useful. For example, it seems interesting to investigate whether the presented theory – under certain constraints – might generate (series of) integers with interesting properties (such as high valued prime numbers) or if it could be able to describe diffusion along a BB-like surface or the migration of randomly moving animals. Also: If some company would start a roulette like game based on random movements along BB edges the here presented theory could be of great help to make a fortune. Or, if people start, as a variant to the board game Go, such a game on the 60 sites of a BB. Further: One might meet the problem of finding the next numbers in the following puzzle sequences:

Sequence 1: 1 0 3 0 15 2 91 28 607

Sequence 2: 0 0 0 0 0 1 1 20 23 271,

which are 306 and 355, respectively, as is seen from the results presented in sect. IV.

The readers of this work are encouraged to think about the above and other applications of presented approach.

The rest of this paper is organized as follows. As a starter for the interested reader a not too comprehensive introduction to the TBM, assuming an Hamiltonian $\mathcal{H}$ representing next-neighbour interactions between the site functions, and the basics of GT is given, in section II. These basics are used in section III with derivations of the expressions for the (spread-out or delocalized) eigenfunctions of the BB. The transformation between site and eigenfunctions are introduced and analytical expressions for the NoWs and NoVs are presented. Computational results of the latter are shown and discussed in section IV, together with a note on the numerical accuracy. The paper end with concluding remarks: section V.

II. Basic theory: Tight Binding model and Group Theory

This section discusses in short the principles of the TB model (TBM) and how it can be used to compute the number of ways (NoWs) to travel between two given sites in a given number of steps: the NoWs equation. A simple example will be discussed in some detail which also will be used to illustrate the basic principles of GT in a subsection II.2.

II.1 The Tight Binding Model

In this paper we will use the so-called bra-ket notation to deal with functions, operators and overlap between the functions (site functions or linear combinations thereof). In the TBM the initial functions are *site-localized* functions which are here denoted, considering a ket, by $|n\rangle$, with *n* denoting a certain site. These functions are chosen to be ortho-normalized according to

$$\langle n|m\rangle = \delta_{nm},$$

with δ_m the Kronecker delta. We assume only nearest neighbour interaction (nn) between these functions, which then leads to:

$$\mathcal{H} \equiv \sum_{n,m}^{N} t\left(|n\rangle\langle m| + |m\rangle\langle n|\right)_{n \text{ is nn of } m}, \tag{1}$$

with $\mathcal{H}$ the Tight Binding (TB) Hamiltonian (TBH). It is seen that the operator is symmetric as

$$\langle n|\mathcal{H}|m\rangle = \langle m|\mathcal{H}|n\rangle .$$

The eigenfunctions corresponding to the TBH are denoted by

$$|\chi_p\rangle = \sum_{n=1}^{N} V_{pn}|n\rangle, \ \langle \chi_m \mid \chi_p \rangle = \delta_{mp}, \tag{2}$$

and can be chosen to be real and orthonormal owing to $\mathcal{H}$ being a symmetric operator. The above implies the following

$$\sum_{m=1}^{N} |\chi_m\rangle\langle\chi_m| = 1, \tag{3}$$

due to the completeness of the (orthonormal) set.

The eigenvalue corresponding to the above is denoted by

E_m, with $\mathcal{H}|\chi_m\rangle \equiv E_m|\chi_m\rangle$.

Now we are ready to introduce the basic expression for the NoWs for considered system:

$$\begin{aligned} W_{l,m}^{(M)} &\equiv \langle l|\mathcal{H}^M|m\rangle_{t=1} = \sum_{p=1}^{N} \langle l|\mathcal{H}^M \mid \chi_p\rangle\langle\chi_p|m\rangle = \sum_{p=1}^{N} \langle l|\chi_p\rangle E_p^M \langle\chi_p|m\rangle \\ &= \sum_{p=1}^{N} V_{pl} V_{pm} E_p^M, \end{aligned} \tag{4}$$

where eq. 3 was used for the second equality, the eigenvalue equation for the third equality, and $W_{l,m}^{(M)}$ is the number of ways to travel form site *l* to site *m* in *M* steps. The latter follows from the observation that the operator $\mathcal{H}$, in its action on a certain site function $|n\rangle$, generates all the functions of neighbouring sites of site *n*, according to eq. 1, and so corresponds to one step from site *n* to all neighbouring site. Similarly, $\mathcal{H}^M|n\rangle$ generates all possible functions on sites that can be reached in *M* steps starting from site *n*. The final expressions in eq. 4 shows immediately the advantage of the approach for large values of *M*: the NoWs can be evaluated in one single step, needing no (possibly complicated) bookkeeping. It is seen that the quantity $W_{l,m}^{(M)}$ is symmetric for interchanging *l* and *m*, as expected owing to the nature of the operator $\mathcal{H}$, and also that $W_{l,m}^{(0)} = \delta_{lm}$, owing to the orthonormalized site functions.

For later use we note that matrix $\boldsymbol{V}$, introduced in eq. 2, should be unitary by the scaling leading to eq. 3, and the symmetry of the matrix associated with $\mathcal{H}$, $\boldsymbol{H}$, with

$$H_{mn} \equiv \langle m|\mathcal{H}|n\rangle,$$

according to eq. 1. The unitarily of $\boldsymbol{V}$ is a property rather well-known from matrix theory, as well as the following

$$\boldsymbol{V}^t = \boldsymbol{V}^{-1}, \ \boldsymbol{D} = \boldsymbol{V}^{-1}\boldsymbol{H}\boldsymbol{V} . \tag{5}$$

In the above the superscript *t* denotes the transpose, superscript –1 the inverse and $\boldsymbol{D}$ is a diagonal matrix with the eigenvalues of $\boldsymbol{H}$ being the diagonal entries.

As an illustration to the above, and also as an onset of the group theoretical considerations discussed later on, we first consider a closed, *regular* chain with *N* interacting sites; it will also be used later on to consider the stand-alone first (N=5) and second (N=15) girdles of the BB (see fig. 1).

We try orthonormal eigenfunctions of the Hamiltonian defined by eq. 1 of the form

$$|\varphi_m\rangle = {}^{1}\!/\!_{\sqrt{N}} \sum_{l=1}^{N} e^{ia_m l} |l\rangle,\ l,m = 1:N, \text{ with } a_m \equiv 2m\pi / N\ , \tag{6}$$

The TB interaction involves nearest neighbours only so that, e.g., site 2 interacts with sites 1 and 3, site 1 with site N and 2 (and vice versa). Careful bookkeeping leads to

$$\mathcal{H}|\varphi_m\rangle = {}^{t}\!/\!_{\sqrt{N}} \sum_{l=1}^{N} \left(e^{ia_m} + e^{-ia_m}\right) e^{ia_m l} |l\rangle = \hat{E}_m |\varphi_m\rangle;\ \hat{E}_m \equiv 2t\cos a_m\,, \tag{7}$$

where the circumflex designates the temporary numbering of the eigenstates from the definite one, introduced below.

So, the eigenvalues for the case $N = 5$ are given as follows:

$$\begin{aligned} &\hat{E}_1, \hat{E}_4 = 2t\cos a_1 = 2t(\sqrt{5}-1)/4 = 0.6180t \\ &\hat{E}_2, \hat{E}_3 = 2t\cos 2a_1 = 2t(-1-\sqrt{5})/4 = -1.6180t \\ &\hat{E}_5 = 2t \end{aligned} \tag{8}$$

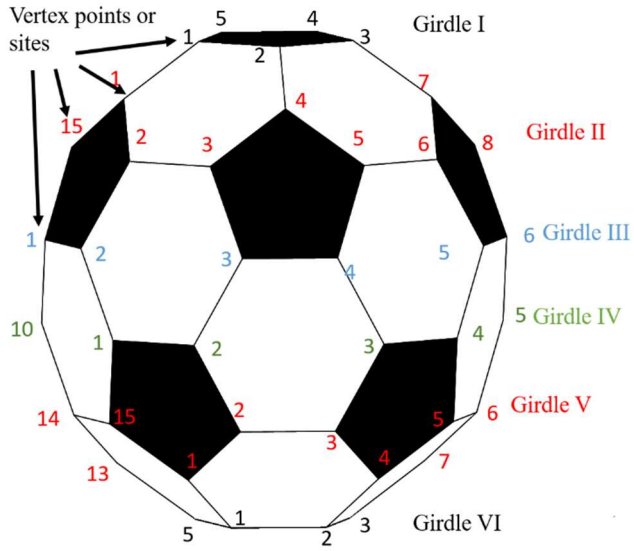

Figure 1. *Picture of a BB, showing part of the facets and the applied subdivision of the 60 vertex points into six girdles with indicated site numbering.*

It is seen from eq. 8 that there are two two-fold degenerate states and one singlet state, which is (in considered case) the fully symmetric state, which corresponds to an eigenfunction consisting of the sum of all site functions with real – by choice – and equal amplitudes ($1/\sqrt{5}$). The other eigenfunctions can be made real – which may ease both notation and computations – by using, e.g., that $|\varphi_1\rangle = |\varphi_4^*\rangle$ (with * denoting the complex conjugate) and choosing

$$|\psi_1^I\rangle + i|\psi_2^I\rangle = \left(|\varphi_1\rangle + |\varphi_4\rangle\right)/\sqrt{2} + i\,\mathrm{Im}\left(|\varphi_1\rangle - |\varphi_4\rangle\right)/\sqrt{2}\,, \tag{9}$$

Note that the new eigenfunctions have been re-numbered. Similarly, $|\psi_3^I\rangle$ and $|\psi_4^I\rangle$ are introduced from $|\varphi_2\rangle$ and $|\varphi_3\rangle$; for consistency in notation we choose $|\psi_5^I\rangle = |\varphi_5\rangle$. Applying the same re-ordering to the eigenvalues it follows:

$$E_{1:5} = t[(\sqrt{5}-1)/2;\ (\sqrt{5}-1)/2;\ -(\sqrt{5}+1)/2;\ -(\sqrt{5}+1)/2;\ 2]\,. \tag{10}$$

With these choices we can present the entries of the unitary matrix, V^I, representing in its columns the eigenvectors expressed in terms of the site-amplitudes:

$$\boldsymbol{V}^I = \sqrt{\frac{2}{5}} \begin{array}{c} \begin{matrix} \left|\psi_1^I\right\rangle & \left|\psi_2^I\right\rangle & \left|\psi_3^I\right\rangle & \left|\psi_4^I\right\rangle & \left|\psi_5^I\right\rangle \end{matrix} \\ \begin{pmatrix} C_1 & S_1 & C_2 & S_2 & w \\ C_2 & S_2 & C_4 & S_4 & w \\ C_3 & S_3 & C_1 & S_1 & w \\ C_4 & S_4 & C_3 & S_3 & w \\ 1 & 0 & 1 & 0 & w \end{pmatrix} \end{array} \begin{matrix} \left|1^I\right\rangle \\ \left|2^I\right\rangle \\ \left|3^I\right\rangle \\ \left|4^I\right\rangle \\ \left|5^I\right\rangle \end{matrix} \qquad \begin{matrix} C_m = \cos(2\pi m/5) \\ S_m = \sin(2\pi m/5) \\ m = 1-4 \\ w \equiv 1/\sqrt{2} \end{matrix} \tag{11}$$

with the superscript I denoting that the expressions concern the I^{st} girdle.
The results of the TB Model (TBM) can directly be used to find transparent and easy to evaluate expressions for the NoWs to travel in a given number of steps M between two sites of considered regular structure, like considered pentagon. The corresponding quantity, W, is given by

$$, \qquad W_{l,m}^{(M)} \equiv \left\langle l^I \left| \boldsymbol{\mathcal{H}}_I^M \right| m^I \right\rangle_{t=1} \tag{12}$$

with – as indicated – $t=1$, which is the assumed value for t from here on, unless stated otherwise, and $\boldsymbol{\mathcal{H}}_I$ denotes that the (stand-alone) 1st girdle is considered. Taking into account that $\left|\psi_p^I\right\rangle,\ p=1:5$ forms a complete orthonormal set it follows:

$$W_{l,m}^{(M)} = \sum_{p=1}^{5} \left\langle l^I \left| \psi_p^I \right\rangle E_p^M \left\langle \psi_p^I \right| m^I \right\rangle . \tag{13}$$

As an example to the above we give expressions and corresponding values for $W_{l,m}^{(M)}$ for the indicated value of M with $l=m=1$ and $l=1,\ m=3$, leading to

$$\left.\begin{aligned} W_{1,1}^{(M)} &= \sum_{p=1}^{5} V_{1p}^I V_{1p}^I E_p^M = \quad 1,0,2,0,6,2,215492564 \\ W_{1,3}^{(M)} &= \sum_{p=1}^{5} V_{1p}^I V_{3p}^I E_p^M = 0,0,1,1,4,5,214978335 \end{aligned}\right\} M = 0,..,5,30. \tag{14}$$

The results are, as anticipated, confirming orthonormality of the row vectors of matrix $\boldsymbol{V}$ (as is seen from the results in eq. 14 for M=0) and the correct number of different ways to travel for the cases M = 1-5, checked by counting; the case M = 30 was not checked in such a way by us for obvious reasons. The deviations of these NoWs from the corresponding integers was $\delta W \approx 10^{-16}$ (M=0-5) and $\delta W \approx 10^{-8}$ (M=30); note the more general relation: $\delta W / W \approx 10^{-16}$.
With rather simple reasoning, one may prove:

$$W_{l,m}^{(M)} \propto 2^M/5 \text{ if } M \to \infty \text{ and } W_{l,l}^{(M+1)} = 2W_{l,l\pm 1 \bmod 5}^{(M)} . \tag{15}$$

The first equality follows for example from eq. 13 also using that there is only one largest eigenvalue – in absolute sense – of $\boldsymbol{\mathcal{H}}_1$, one with value 2 ($t=1$), which becomes dominant for large M. The second one may be proved, by the interested reader, using the equations above (numerically or (lengthier) analytically) or by arguing.

II.2 Group Theory

Below only the most elementary features of (point) group theory will be presented; for more details the interested reader is referred to the huge amount of literature on the topic (see e.g. [I-V], but there is much more). We will summarize only as much as is needed for the derivations given in section III.
A point group consists of all the symmetry operations or a well-chosen part thereof, all having a fixed point in common, that can be performed on a planar or spatial entity (like a molecule or a Bucky ball having a certain symmetry) that result in a conformation being indistinguishable from the original. The phrase 'or a well-chosen part thereof' means that used symmetry does

not have to be the full symmetry, one may limit himself or herself to a certain symmetric aspect (in this section the fivefold rotation).

Below, we will consider the so-called C_{5v} point group – relevant for both the above discussion on the TBM and that in sect. III – to illustrate things. In table I – showing a so-called *character table* – the first horizontal line shows the name of the point group as well as symbols for its symmetry operations which are ordered in so-called conjugacy classes [I-II] being: E, the identity operation; C_5, rotation over an angle of $\pm a_1 \equiv \pm 2\pi/5$ (owing to the five-fold rotation axis), with a_1 also defined in eq. 6; C_5^2 rotation over an angle of $\pm a_2 \equiv \pm 4\pi/5$; σ_v mirroring across a line or plane. The reason for the introduction of classes will be discussed below; the number of operations in each class are also indicated in the first line of the table (1, 2, 2, 5 respectively). The sum of these numbers is the order of the point group, h (=10).

The first horizontal line displays the so-called irreducible representations (IRs) with interesting properties discussed in the pages to follow. The table *entries* consist of characters, the traces of the matrices representing group elements of the column's class in the given row's group representation.

$\mathbf{C_{5v}}$	E	$2C_5$	$2C_5^2$	$5\sigma_v$
$\boldsymbol{a}_1$	1	1	1	1
$\boldsymbol{a}_2$	1	1	1	–1
$\boldsymbol{\varepsilon}_1$	2	$2\cos(2\pi/5)$	$2\cos(4\pi/5)$	0
$\boldsymbol{\varepsilon}_2$	2	$2\cos(4\pi/5)$	$2\cos(2\pi/5)$	0

Table I. Character table for the C_{5v} point group, with irreducible representations (IRs) $\boldsymbol{a}_1$, $\boldsymbol{a}_2$, $\boldsymbol{\varepsilon}_1$, $\boldsymbol{\varepsilon}_2$, conjugacy classes E, C_5, C_5^2 *and* σ_v *and order (number of symmetry operations)* $h = 10$ *;* $2\cos(2\pi/5) = 0.6180,\ 2\cos(4\pi/5) = -1.6180$.

One may introduce a number of (spatial or planar) domains, distributed according to the point group symmetry, with on each such a domain one or more functions (like orbitals in a regular molecule). For the C_{5v} point group for example the number of functions should then be a multiple of five. If one also assumes that these functions interact according to the symmetry of the group (i.e., corresponding to an operator which is invariant under group operations, e.g., an operator as in eq. 1) the resulting eigenstates will be singlets or degenerate states, for which certain properties hold. A number of these are quite relevant for the aimed computations and will be discussed next. No proofs will be given; for these the reader is referred to the literature [I-V].

Group theoretical properties

1. Most of the eigenfunctions corresponding to a group-symmetric operator will not have the full symmetry of the group, but the result of any symmetry operation of the group on such an eigenfunction will also be an eigenfunction to considered operator, generally (but not always) differing from the original one.
2. The eigenfunctions can be subdivided according to their behaviour under group operations into so-called irreducible representations (IRs). The order of these IRs can be unity or higher (the latter corresponding to degenerate states). The result of a group operation working on such a function belonging to a certain IR can be written as the linear combination of all functions of the same IR.
3. For the C_{5v} point group these IRs are denoted by $\boldsymbol{a}_1$, $\boldsymbol{a}_2$, $\boldsymbol{\varepsilon}_1$, and $\boldsymbol{\varepsilon}_2$ (see Table I).

4. All point groups have one IR with corresponding function(s) that remain unchanged under group operations, implying that these functions have the full group symmetry. Such an IR is usually denoted by $\boldsymbol{a}_1$.
5. Under group operations the transformation of functions belonging to a certain IR can be described by a (square) matrices (one for each operation, all being of the same order as considered IR). As a consequence of this the *character* or *trace* corresponding to the identity operation, E, is the order of the IR (see e.g. the second column of table I). Examples of how to compute such a trace will be given below (see eqs. 18 and 19).
6. The sum of the squared orders of all IRs is equal to the order of the group, h (= 10 = $1^2 + 1^2 + 2^2 + 2^2$)
7. The characters of the matrices representing the group operations of a certain class for functions corresponding to a certain IR are all the same.
8. Any *operator*, say $\mathcal{H}_A$, having the full symmetry of the point group (implying a symmetry according to IR $\boldsymbol{a}_1$) induces an interaction between functions of the *same* IR type only, thus generating new solutions of the same IR type (this also means degeneracy, if present, is maintained).
9. For states belonging to such degenerate IRs things can be arranged such that for group-symmetric operators the interactions between the functions of different levels but belonging to the same IR type are one-by-one. This can be done – for each couple of function sets – via similarity transformations (or reorientations) adapting the functions of one of such set, and may repeated for all other sets, if desired. Once this has been done this situation is maintained even if new – full symmetric – operators would become into play.
10. Sets which all have the same 'orientation' (i.e. having one by one interaction via fully symmetric operators) can *all* be reoriented with respect to a new set (of the same IR type) by the *same* similarity transformation. The above one by one interaction enables the separation of functions of doubly degenerate states into α and β states with interactions due to group-symmetric Hamiltonians only exclusively among α states and exclusively among β states.

The so-called reorientation procedure is detailed in the Appendix where also suggestions for its numerical implantation are presented.

The introduction of α and β states above is illustrated below by repeating eq. 11, but now also indicating the corresponding functions of the α and β type.

$$\begin{array}{c} \left|\psi_1^I\right\rangle\left|\psi_2^I\right\rangle\left|\psi_3^I\right\rangle\left|\psi_4^I\right\rangle\left|\psi_5^I\right\rangle \\ \boldsymbol{V}^I = \sqrt{\frac{2}{5}}\begin{pmatrix} C_1 & S_1 & C_2 & S_2 & w \\ C_2 & S_2 & C_4 & S_4 & w \\ C_3 & S_3 & C_1 & S_1 & w \\ C_4 & S_4 & C_3 & S_3 & w \\ 1 & 0 & 1 & 0 & w \end{pmatrix} \begin{array}{c} \left|1^I\right\rangle \\ \left|2^I\right\rangle \\ \left|3^I\right\rangle \\ \left|4^I\right\rangle \\ \left|5^I\right\rangle \end{array} \\ \begin{array}{ccccc} \alpha & \beta & \alpha & \beta & \\ \nwarrow & \nearrow & \nwarrow & \nearrow & \uparrow \\ \text{IRs:} & \boldsymbol{\varepsilon}_1 & & \boldsymbol{\varepsilon}_2 & \boldsymbol{a}_1 \end{array} \end{array}$$

Note that properties above imply that, considering a structure with a certain symmetry, an eigenvalue problem with a large number of interacting states can be split – according to their

IRs – into a few (much) smaller problems, each with less functions involved, as there will be no interactions between functions of different representations and for degenerate IRs advantage can be taken from the above (points 9 and 10) mentioned one-by-one interactions between different states, as discussed and demonstrated for the specific case of this paper in more detail below.
There is much more to say about group theory than presented here(see the rich literature on the topic, e.g. [I-V]), but the above is what we will need for this presentation.

III. Main Theory

III.1 Computational approach

The splitting of the Hamiltonian of the complete BB, $\mathcal{H}$, into sub-operators is given by eq. 16, with subscripts *N* and *S* referring to northern and southern hemisphere, respectively, the subscript NS indicates the interaction between girdles III and IV and so between the two hemispheres. For symmetry reasons there is a one to one correspondence between the two; so only $\mathcal{H}_N$ – of which the solutions will be considered explicitly – is split into the here considered sub-Hamiltonians in eq. 16. It is the sum of the Hamiltonian for the three stand-alone girdles *I-III* and the interactions between the first and the second girdles and between the second and third girdles, denoted by $\mathcal{H}_1$ and $\mathcal{H}_2$, respectively. Once the eigenvalues and eigenfunctions of $\mathcal{H}_N$ are known, these results can be used also for the southern hemisphere, owing to symmetry, after which the two solutions can be coupled via $\mathcal{H}_{NS}$ which describes basically the coupling between girdles *III* and *IV*.

$$\mathcal{H} = \mathcal{H}_N + \mathcal{H}_S + \mathcal{H}_{NS};\ \mathcal{H}_N = \mathcal{H}_I + \mathcal{H}_{II} + \mathcal{H}_{III} + \mathcal{H}_1 + \mathcal{H}_2;\quad \mathcal{H}_1 : I \leftrightarrow II,\ \mathcal{H}_2 : II \leftrightarrow III \tag{16}$$

Explicit expressions of the sub-Hamiltonians will be given below.

III.2 Girdle I

The first girdle has already been considered in considerable detail in section II. Now we are able to discuss group theoretical aspects of the eigenstates corresponding to the Hamiltonian $\mathcal{H}_I$. In particular the corresponding IRs will be identified using the character table of the C_{5v} point group given above.
With the aid of the expressions for the eigenfunctions, eq. 11, it follows immediately that the fifth state corresponds to the $\mathcal{A}_1$ IR: the eigenfunction of that state does not change under any of the group operations.
The IRs of the two doubly degenerate states can be determined as will be demonstrated for functions (of eq. 11). We consider a rotation over an angle of $2\pi/5$ (one of the group operations; it is leading to a cyclic permutation of the site functions such that the site function 2 moves to site 1 etc.). The operation can be denoted by:

$$\begin{pmatrix} \tilde{\psi}_1 \\ \tilde{\psi}_2 \end{pmatrix} = \boldsymbol{M} \begin{pmatrix} \psi_1 \\ \psi_2 \end{pmatrix}, \tag{17}$$

with $\boldsymbol{M}$ an 2x2 matrix and with the tilde (~) indicating the effect of considered rotation. Using orthonormality of the function involved we arrive at the expression for the trace:

$$T_{C_5} = M_{11} + M_{22} = \langle \tilde{\psi}_1 \,|\, \psi_1 \rangle + \langle \tilde{\psi}_2 \,|\, \psi_2 \rangle = \tilde{\boldsymbol{V}}^I_{:,1} \cdot \boldsymbol{V}^I_{:,1} + \tilde{\boldsymbol{V}}^I_{:,2} \cdot \boldsymbol{V}^I_{:,2}, \tag{18}$$

The final expression in the above contains vectorial symbols for the eigenfunctions (see also eq. 11) $\boldsymbol{V}^{I}_{:,p}$, $p=1,2$ which are specified below

$$T_{C_5} = \overbrace{\sqrt{\frac{2}{5}}\begin{pmatrix}\cos a_2\\ \cos a_3\\ \cos a_4\\ 1\\ \cos a_1\end{pmatrix}}^{\tilde{V}^{I}_{:,1}} \bullet \overbrace{\sqrt{\frac{2}{5}}\begin{pmatrix}\cos a_1\\ \cos a_2\\ \cos a_3\\ \cos a_4\\ 1\end{pmatrix}}^{V^{I}_{:,1}} + \overbrace{\sqrt{\frac{2}{5}}\begin{pmatrix}\sin a_2\\ \sin a_3\\ \sin a_4\\ 0\\ \sin a_1\end{pmatrix}}^{\tilde{V}^{I}_{:,2}} \bullet \overbrace{\sqrt{\frac{2}{5}}\begin{pmatrix}\sin a_1\\ \sin a_2\\ \sin a_3\\ \sin a_4\\ 0\end{pmatrix}}^{V^{I}_{:,2}} = 2\cos a_1;\ a_m \equiv 2m\pi/5\,. \quad (19)$$

The result implies, as is seen with table I, that we have to do with an $\mathcal{E}_1$ IR. Similarly, it may be derived that the second degenerate state of the considered pentagon has $\mathcal{E}_2$ symmetry.

III.3 The second girdle

Next the second girdle with fifteen vertices is considered with interactions between site functions of neighbouring vertices on that girdle, according to Hamiltonian $\mathcal{H}_{II}$. The expressions for eigenvectors and corresponding eigenvalues are given by eqs. 6 and 7 (with N = 15). The latter ones can be expressed as

$$\begin{aligned}\hat{E}^{II}_{1,14} = 2\cos b_1;\ \hat{E}^{II}_{2,13} = 2\cos b_2;\ \hat{E}^{II}_{3,12} = 2\cos b_3;\ \hat{E}^{II}_{4,11} = 2\cos b_4;\ \hat{E}^{II}_{5,10} = 2\cos b_5;\\ \hat{E}^{II}_{6,9} = 2\cos b_6;\ \hat{E}^{II}_{7,8} = 2\cos b_7;\ \hat{E}^{II}_{15} = 2;\ b_m \equiv 2m\pi/15\end{aligned} \quad (20)$$

where the circumflex indicates that the ordering is only temporarily. Next linear combinations of functions corresponding to the same energy level are made such that the results are all real functions, similarly as above (see eq. 9). The degenerate states are given in the following set of pairs:

$$1,14;\ 2,13;\ 3,12;\ 4,11;\ 5,10;\ 6,9;\ 7,8\,, \quad (21)$$

which correspond to IRs $\mathcal{E}_1$ or $\mathcal{E}_2$ or 'accidently' degenerate of $\mathcal{A}_1$ or $\mathcal{A}_2$ symmetry, as discussed next. The singlet state (having label 15) will be a $\mathcal{A}_1$ state, as shown below.

The IRs corresponding to above solutions can be found by using table I, similarly as for the solutions of the first girdle. The following strategy has been used:

- The twofold *degenerate* states are checked considering again a rotation over angle of $2\pi/5$ followed by a computation of the trace. This required process is basically as above, leading to eq. 19, but now the vectors have fifteen entries. The evaluation of the traces can most conveniently be done numerically. IRs $\mathcal{E}_1$ and $\mathcal{E}_2$ are recognized immediately. If the computed trace is equal to 2, implying that one has to do with accidently degenerate states of IR $\mathcal{A}_1$ or $\mathcal{A}_2$, an extra check is needed, as follows.
- The aforementioned (real) functions are checked one by one computing the effect of mirroring (one of the five σ_v operations), followed by computation of the inner product (the character) between initial and resulting vectors (see as an example eqs. 18 and 19), and comparing the result with the entries of table I. A more simple alternative is based on checking the fifteen vector entries in order to choose between IRs $\mathcal{A}_1$ and $\mathcal{A}_2$,. For the $\mathcal{A}_1$ IR these fifteen entries are cyclic with a period of three (so the function has group symmetry); this does not hold for eigenfunctions with $\mathcal{A}_2$ symmetry. It is found that the states with labels 5, 10 (which are 'accidently' degenerate) and 15 all have $\mathcal{A}_1$ symmetry.

We arrive at results given in table II. It was found that there are no $\mathcal{A}_2$ IRs present, which we attribute to the nature of used Hamiltonian, $\mathcal{H}_{II}$.

Represent.	***Energies***	***Energies*** *(renumbered)*	***Eigenfunctions***
$\mathcal{E}_1$	$\hat{E}^{II}_{1,14}, \hat{E}^{II}_{4,11}, \hat{E}^{II}_{6,9}$	$E^{II}_{1,2}, E^{II}_{3,4}, E^{II}_{5,6}$	$\left\|\psi^{II}_{1-6}\right\rangle$
$\mathcal{E}_2$	$\hat{E}^{II}_{2,13}, \hat{E}^{II}_{3,12}, \hat{E}^{II}_{7,8}$	$E^{II}_{7,8}, E^{II}_{9,10}, E^{II}_{11,12}$	$\left\|\psi^{II}_{7-12}\right\rangle$
$\mathcal{A}_1$	$\hat{E}^{II}_{5,10}, \hat{E}^{II}_{15}$	$E^{II}_{13}, E^{II}_{14}, E^{II}_{15}$	$\left\|\psi^{II}_{13-15}\right\rangle$

Table II. *Irreducible representations of the second girdle consisting of fifteen sites assuming tight binding interactions within this girdle only as well as the chosen re-numbering of the eigenstates ordered according to their representations.*

To keep things simple a re-numbering as above (for the functions of girdle II) is applied. It is convenient to apply a similarity transformation on the functions of the degenerate IRs $\mathcal{E}_1$ and $\mathcal{E}_2$, as mentioned under points 9 and 10 in sect. II, leading to *one by one* interactions (via $\mathcal{H}_1$) with corresponding states of girdle I. An example of mentioned treatment is given next for a state with $\mathcal{E}_1$ symmetry, with eigenvalues and eigenfunctions $\hat{E}^{II}_{1,14}$, $\hat{\varphi}^{II}_1$ and $\hat{\varphi}^{II}_{14}$.
The new eigenfunctions are then calculated as explained in the Appendix. First applying a renumbering followed determination of $\eta(=\pm 1)$:

$$\varphi^{II}_1 = \hat{\varphi}^{II}_1,\ \varphi^{II}_2 = \hat{\varphi}^{II}_{14};\ \eta = \mathrm{sgn}(I_{11}/I_{22}),\quad I_{lm} \equiv \left\langle \psi^{I}_m \middle| \mathcal{H}_1 \middle| \varphi^{II}_l \right\rangle;\ l,m = 1,2, \tag{22}$$

and the renumbering is denoted by omitting the circumflex (^) above symbols. The similarity transformation is then given by:

$$\begin{pmatrix} \psi^{II}_1 \\ \psi^{II}_2 \end{pmatrix} = \begin{pmatrix} \cos\theta & \eta\sin\theta \\ -\sin\theta & \eta\cos\theta \end{pmatrix} \begin{pmatrix} \varphi^{II}_1 \\ \varphi^{II}_2 \end{pmatrix};\ \theta \equiv \tan^{-1}\left(\frac{I_{12}}{I_{11}}\right). \tag{23}$$

It is seen that, according to eq. 23 the following holds (for example):

$$\left\langle \psi^{I}_1 \middle| \mathcal{H}_1 \middle| \psi^{II}_2 \right\rangle = \sin\theta I_{11} + \cos\theta I_{12} = 0,$$

and so, because, according to the statements of properties 9 and 10 in sect. II, the matrix in eq. 23 defines the sought similarity transformation. So, (in summary) the following relations hold according to above formulae:

$$\left\langle \psi^{II}_1 \middle| \mathcal{H}_1 \middle| \psi^{I}_1 \right\rangle = \left\langle \psi^{II}_2 \middle| \mathcal{H}_1 \middle| \psi^{I}_2 \right\rangle;\ \left\langle \psi^{II}_1 \middle| \mathcal{H}_1 \middle| \psi^{I}_2 \right\rangle = \left\langle \psi^{II}_2 \middle| \mathcal{H}_1 \middle| \psi^{I}_1 \right\rangle = 0. \tag{24}$$

The eigenfunctions in table II can – after all having been reoriented, similarly as above – be straightforwardly expressed in terms of the fifteen site functions of girdle II in a similar way as for the first girdle (see eq. 11) by the unitary matrix V^{II} (nor given here), with

$$V^{II}_{ml} \equiv \left\langle m^{II} \middle| \psi^{II}_l \right\rangle,\ m,l = 1-15. \tag{25}$$

III.4 The third girdle

In fig. 1 it is seen that the third girdle consists of ten vertices which are coupled by the TBH $\mathcal{H}_{III}$ in five pairs (starting at sites numbered with 1 and 2); there is no interaction between the functions of, for example, sites 2 and 3, because of the larger distance between the two. Considering the first pair it is simply seen that the corresponding eigenvalues and functions, owing to the TB interactions, are given by:

$$\left|\varphi^{III}_{1+}\right\rangle = 1/\sqrt{2}\left(\left|1\right\rangle^{III} + \left|2\right\rangle^{III}\right),\ \left|\varphi^{III}_{1-}\right\rangle = 1/\sqrt{2}\left(\left|1\right\rangle^{III} - \left|2\right\rangle^{III}\right),\ \hat{E}^{III}_{1+} = t,\ \hat{E}^{III}_{1-} = -t. \tag{26}$$

Also taking into account the other pairs it follows that there are five pairs with energy t and five with energy $-t$. So, there are only two (five-fold degenerate) energy levels from which the different IRs cannot be identified easily. But, considering either one of these two sets of pairs, say the one with the + as subscript, the situation makes us think on the solution for girdle I, with also a fivefold symmetry (see sect. II.1, eq. 11). As to girdle III, assuming no interaction with neighbouring girdles, there is no (direct) interaction between the five function pairs (with given TBH). The idea is that the solutions for girdle III should look like those of girdle I, and the entries of the first two columns in eq. 11 (corresponding to the IR $\mathcal{E}_1$) will be used to define the coefficients for the five function pairs of the type given in eq. 26 with both the + and – sign for the two $\mathcal{E}_1$ IRs of girdle III. So, to that end we will try the following two sets, as a starting point:

$$\left.\begin{array}{l} \left|\bar{\psi}_1^{III}\right\rangle = 1/\sqrt{5}\left(C_1\ C_1\ C_2\ C_2\ C_3\ C_3\ C_4\ C_4\ 1\ 1\right)^t \\ \left|\bar{\psi}_2^{III}\right\rangle = 1/\sqrt{5}\left(S_1\ S_1\ S_2\ S_2\ S_3\ S_3\ S_4\ S_4\ 0\ 0\right)^t \end{array}\right\} \mathcal{E}_1,\ \text{energy: } t$$

$$\left.\begin{array}{l} \left|\bar{\psi}_3^{III}\right\rangle = 1/\sqrt{5}\left(C_1\ -C_1\ C_2\ -C_2\ C_3\ -C_3\ C_4\ -C_4\ 1\ -1\right)^t \\ \left|\bar{\psi}_4^{III}\right\rangle = 1/\sqrt{5}\left(S_1\ -S_1\ S_2\ -S_2\ S_3\ -S_3\ S_4\ -S_4\ 0\ 0\right)^t \end{array}\right\} \mathcal{E}_1,\ \text{energy: } -t \qquad (27)$$

The correctness of the indicated IR can easily be checked by using the character table. The bar above the functions indicates that a reorientation step still has to take place to realize one-to-one interactions with the $\mathcal{E}_1$ IRs of girdle II (using only one of these girdle II solutions is enough according to property 10 in sect. III.1). The result is presented in the first four columns of eq. 28, given below. Similarly the functions for the $\mathcal{E}_2$ (also two sets) and $\mathcal{A}_1$ (two states) IRs are defined.

$$\boldsymbol{V}^{III} = \sqrt{\frac{1}{5}} \begin{array}{c} \begin{array}{cccccccccc} \left|\psi_1^{III}\right\rangle & \left|\psi_2^{III}\right\rangle & \left|\psi_3^{III}\right\rangle & \left|\psi_4^{III}\right\rangle & \left|\psi_5^{III}\right\rangle & \left|\psi_6^{III}\right\rangle & \left|\psi_7^{III}\right\rangle & \left|\psi_8^{III}\right\rangle & \left|\psi_9^{III}\right\rangle & \left|\psi_{10}^{III}\right\rangle \end{array} \\ \begin{pmatrix} C_1 & S_1 & -S_1 & C_1 & C_2 & S_2 & S_2 & -C_2 & w & w \\ C_1 & S_1 & S_1 & -C_1 & C_2 & S_2 & -S_2 & C_2 & w & -w \\ C_2 & S_2 & -S_2 & C_2 & C_4 & S_4 & S_4 & -C_4 & w & w \\ C_2 & S_2 & S_2 & -C_2 & C_4 & S_4 & -S_4 & C_4 & w & -w \\ C_3 & S_3 & -S_3 & C_3 & C_1 & S_1 & S_1 & -C_1 & w & w \\ C_3 & S_3 & S_3 & -C_3 & C_1 & S_1 & -S_1 & C_1 & w & -w \\ C_4 & S_4 & -S_4 & C_4 & C_3 & S_3 & S_3 & -C_3 & w & w \\ C_4 & S_4 & S_4 & -C_4 & C_3 & S_3 & -S_3 & C_3 & w & -w \\ 1 & 0 & 0 & 1 & 1 & 0 & 0 & -1 & w & w \\ 1 & 0 & 0 & -1 & 1 & 0 & 0 & 1 & w & -w \end{pmatrix} \begin{array}{l} \left|1\right\rangle^{III} \\ \left|2\right\rangle^{III} \\ \left|3\right\rangle^{III} \\ \left|4\right\rangle^{III} \\ \left|5\right\rangle^{III} \\ \left|6\right\rangle^{III} \\ \left|7\right\rangle^{III} \\ \left|8\right\rangle^{III} \\ \left|9\right\rangle^{III} \\ \left|10\right\rangle^{III} \end{array} \\ \begin{array}{cccccccccc} \alpha & \beta & \alpha & \beta & \alpha & \beta & \alpha & \beta & & \end{array} \\ \begin{array}{cccccccccc} \nwarrow & \nearrow & \nwarrow & \nearrow & \nwarrow & \nearrow & \nwarrow & \nearrow & \uparrow & \uparrow \end{array} \\ \begin{array}{cccccccccc} \text{IRs:} & \mathcal{E}_1 & & \mathcal{E}_1 & & \mathcal{E}_2 & & \mathcal{E}_2 & \mathcal{A}_1 & \mathcal{A}_1 \end{array} \end{array} \qquad (28)$$

$$w \equiv 1/\sqrt{2},\ C_m \equiv \cos(2m\pi/5),\ S_m \equiv \sin(2m\pi/5),\ m = 1-4$$

The energies of the corresponding levels are:

$$E^{III}_{1,2,5,6,9} = t,\ E^{III}_{3,4,7,8,10} = -t\ . \qquad (29)$$

III.5 The northern hemisphere

Knowing the energies and eigenfunctions of the three girdles the next step is to consider the interactions between these girdles which form the northern hemisphere of the BB. These are represented by the following Hamiltonians:

$$\begin{aligned}\mathcal{H}_1 &= t\left(\sum_{l=1}^{5}|l\rangle^{I}\langle 3l-2|^{II}+|3l-2\rangle^{II}\langle l|^{I}\right)=t\left(\sum_{l=1}^{5}|l\rangle^{I}\langle 3l-2|^{II}+\text{adjoint}\right)\\ \mathcal{H}_2 &= t\left(\sum_{l=1}^{5}|3l-1\rangle^{II}\langle 2l|^{III}+|3l\rangle^{II}\langle 2l+1\bmod 10|^{III}+\text{adjoint}\right)\end{aligned} \tag{30a}$$

or, less formal but more transparent:

$$\begin{aligned}\mathcal{H}_1 &= t\left(|1\rangle^{I}\langle 1|^{II}+|2\rangle^{I}\langle 4|^{II}+|3\rangle^{I}\langle 7|^{II}+|4\rangle^{I}\langle 10|^{II}+|5\rangle^{I}\langle 13|^{II}+\text{adjoint}\right)\\ \mathcal{H}_2 &= t\begin{pmatrix}|15\rangle^{II}\langle 1|^{III}+|2\rangle^{II}\langle 2|^{III}+|3\rangle^{II}\langle 3|^{III}+|5\rangle^{II}\langle 4|^{III}+|6\rangle^{II}\langle 5|^{III}+|8\rangle^{II}\langle 6|^{III}\\ +|9\rangle^{II}\langle 7|^{III}+|11\rangle^{II}\langle 8|^{III}+|12\rangle^{II}\langle 9|^{III}+|14\rangle^{II}\langle 10|^{III}+\text{adjoint}\end{pmatrix}\end{aligned} \tag{30b}$$

as is seen considering the numbering of sites in fig. 1. In the above expressions 'adjoint' means reversal of the bra and ket operators in foregoing expressions.

In this section we will present expressions for the eigenvalues and eigenfunctions of the TB coupled vertices of the northern hemisphere (NH) of the BB, using earlier results for the three girdles with above Hamiltonians presenting the coupling between these three of the NH. The big advantage of applied group theoretical treatment now becomes clear: The computations can be done separately for the various IRs, and for doubly degenerate IRs the eigenvalue equations hold for pairs of functions for which only one of the equations has to be solved. So, the matrix representing the eigenvalue problem for, for example the $\mathcal{E}_1$ IR, say, $\boldsymbol{M}_{\mathcal{E}_1}^{NH}$, is of an order as low as six (for a problem with thirty functions involved!), and holds for both α and β states (introduced earlier, in sect. II.2). Next, the construction of latter matrix will be given.

So, the interacting functions (of $\mathcal{E}_1$ IRs) are:

$$|\psi_1^{I}\rangle, |\psi_{1,3,5}^{II}\rangle \text{ and } |\psi_{1,3}^{III}\rangle, \tag{31}$$

which can be expressed in terms of site functions as given by eqs. 11 and 31 and following from the recipe leading to eq. 25.

The entries of considered matrix can now be expressed as given below

$$\boldsymbol{M}_{\mathcal{E}_1}^{NH}=\begin{pmatrix} E_1^{I} & M_{12} & M_{13} & M_{14} & 0 & 0\\ M_{12} & E_1^{II} & 0 & 0 & M_{25} & M_{26}\\ M_{13} & 0 & E_2^{II} & 0 & M_{35} & M_{36}\\ M_{14} & 0 & 0 & E_3^{II} & M_{45} & M_{46}\\ 0 & M_{25} & M_{35} & M_{45} & E_1^{III} & 0\\ 0 & M_{26} & M_{36} & M_{46} & 0 & E_2^{III}\end{pmatrix}\begin{matrix}|\psi_1^{I}\rangle\\ |\psi_1^{II}\rangle\\ |\psi_{3,}^{II}\rangle\\ |\psi_5^{II}\rangle\\ |\psi_1^{III}\rangle\\ |\psi_3^{III}\rangle\end{matrix}\quad\begin{matrix}M_{1m}\equiv\langle\psi_1^{I}|\mathcal{H}_1|\psi_m^{II}\rangle=\\ t\sum_{l=1}^{5}V_{l1}^{I}V_{3l-2,2m-3}^{II},\quad m=2,3,4\\ M_{pm}\equiv t\left(\sum_{l=1}^{5}V_{3l-1,2p-3}^{II}V_{2l,2m-9}^{III}\right.\\ +\quad\left.\sum_{l=1}^{5}V_{3l,2p-3}^{II}V_{2l+1\bmod 10,2m-9}^{III}\right),\\ p=2,3,4,\ m=5,6\end{matrix} \tag{32}$$

where we took advantage of its symmetry for the off-diagonal entries. A matrix as above can be used to compute eigenvectors and eigenvalues for the NH of considered IR – using a computational tool – denoted by

$$\boldsymbol{V}^{NH,\mathcal{E}_1} \text{ and } \boldsymbol{E}^{NH,\mathcal{E}_1}, \tag{33}$$

where the first is a matrix and the second a vector, both of order six. As an example we present expressions for the solutions emerging from the interaction according to eq. 32 of both type α and β.These are:

$$\left|\psi_m^{NH,\varepsilon_1,\alpha}\right\rangle = V_{1,m}^{NH,\varepsilon_1}\left|\psi_1^{I}\right\rangle + V_{2,m}^{NH,\varepsilon_1}\left|\psi_1^{II}\right\rangle + V_{3,m}^{NH,\varepsilon_1}\left|\psi_3^{II}\right\rangle + V_{4,m}^{NH,\varepsilon_1}\left|\psi_5^{II}\right\rangle + V_{5,m}^{NH,\varepsilon_1}\left|\psi_1^{III}\right\rangle + V_{6,m}^{NH,\varepsilon_1}\left|\psi_3^{III}\right\rangle$$
$$\left|\psi_m^{NH,\varepsilon_1,\beta}\right\rangle = V_{1,m}^{NH,\varepsilon_1}\left|\psi_2^{I}\right\rangle + V_{2,m}^{NH,\varepsilon_1}\left|\psi_2^{II}\right\rangle + V_{3,m}^{NH,\varepsilon_1}\left|\psi_4^{II}\right\rangle + V_{4,m}^{NH,\varepsilon_1}\left|\psi_6^{II}\right\rangle + V_{5,m}^{NH,\varepsilon_1}\left|\psi_2^{III}\right\rangle + V_{6,m}^{NH,\varepsilon_1}\left|\psi_4^{III}\right\rangle \quad (34)$$
$m = 1-6.$

Here we used that the coefficients $V_{l,m}^{NH,\varepsilon_1}$, $l,m = 1-6$ hold for both the α and β components of the IRs involved (as discussed earlier). The functions ψ in the above can be expressed in site functions with eq. 11 and the treatments leading to eq. 25 and eq. 28.

In a similar way as above one may derive expressions to compute eigenvectors and eigenvalues for the NH corresponding to the representations $\mathcal{E}_2$ and $\mathcal{A}_1$ expressed as

$$\boldsymbol{V}^{NH,\mathcal{E}_2}, \boldsymbol{V}^{NH,\mathcal{A}_1} \text{ and } \boldsymbol{E}^{NH,\mathcal{E}_2}, \boldsymbol{E}^{NH,\mathcal{A}_1}. \quad (35)$$

Being able to compute the eigensolutions for the NH we next consider the solutions for the complete BB (with inclusion of the SH), with 60 interacting sites. But before doing so we point out that one-by-one interactions were obtained for degenerate states, as described above, by a similarity transformations of the functions of girdles II and III, successively, using the properties of eigenfunctions of girdle I as a starting point. If – instead of the latter – a different linear combination of the same functions would have been used the transformed functions of girdles II and III would have changed accordingly. It is important – for the coupling between NH and SH – to realise that such a different set of functions would not have changed the results in eqs. 33 to 35. But, a different choice would have changed – of course – the matrices describing the relation between girdle eigenfunctions and site functions, like $\boldsymbol{V}^I$. So, the results in eqs. 33 to 35 will hold as well for the SH which is spatially identical to the NH, and we may put (for example, for $\mathcal{E}_1$ IRs):

$$\boldsymbol{V}^{SH,\mathcal{E}_1} = \boldsymbol{V}^{NH,\mathcal{E}_1};\ \boldsymbol{E}^{SH,\mathcal{E}_1} = \boldsymbol{E}^{NH,\mathcal{E}_1}. \quad (36)$$

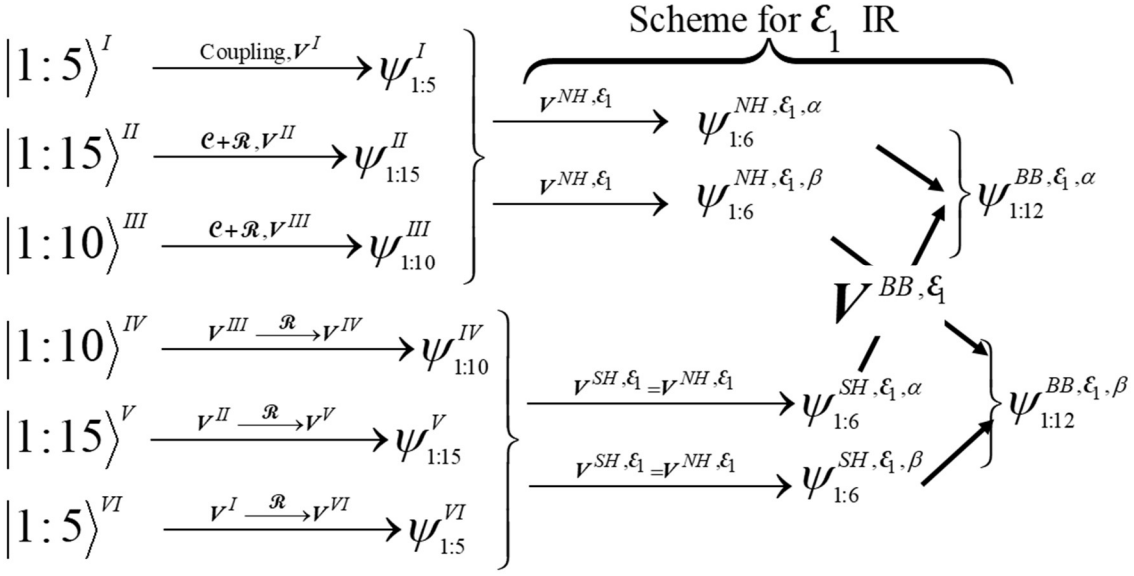

Figure 2. *Full scheme as applied for the coupling between site functions leading to girdle functions which couple, via eigenfunctions for the NH and SH to the final eigenfunctions for the BB. Here only the $\mathcal{E}_1$ IR is considered; the scheme for the $\mathcal{E}_2$ IR is equivalent and that for the $\mathcal{A}_1$ is similar but simpler as only 12 functions are involved, without a subdivision into α and β components. Most symbols have been defined in the text; $\mathcal{C}$ and $\mathcal{R}$ stand for coupling (between the site functions of considered girdle) and reorientation (to obtain one-by-one interaction between two-fold states corresponding to girdle functions (superscripts I-VI); see text), respectively.*

The southern analogue of the expressions in eq. 34 is given by

$$\left|\psi_m^{SH,\varepsilon_1,\alpha}\right\rangle = V_{1,\mathrm{m}}^{SH,\varepsilon_1}\left|\psi_1^{VI}\right\rangle + V_{2,\mathrm{m}}^{SH,\varepsilon_1}\left|\psi_1^{V}\right\rangle + V_{3,\mathrm{m}}^{SH,\varepsilon_1}\left|\psi_3^{V}\right\rangle + V_{4,\mathrm{m}}^{SH,\varepsilon_1}\left|\psi_5^{V}\right\rangle + V_{5,\mathrm{m}}^{SH,\varepsilon_1}\left|\psi_1^{IV}\right\rangle + V_{6,\mathrm{m}}^{SH,\varepsilon_1}\left|\psi_3^{IV}\right\rangle$$
$$\left|\psi_m^{SH,\varepsilon_1,\beta}\right\rangle = V_{1,\mathrm{m}}^{SH,\varepsilon_1}\left|\psi_2^{VI}\right\rangle + V_{2,\mathrm{m}}^{SH,\varepsilon_1}\left|\psi_2^{V}\right\rangle + V_{3,\mathrm{m}}^{SH,\varepsilon_1}\left|\psi_4^{V}\right\rangle + V_{4,\mathrm{m}}^{SH,\varepsilon_1}\left|\psi_6^{V}\right\rangle + V_{5,\mathrm{m}}^{SH,\varepsilon_1}\left|\psi_2^{IV}\right\rangle + V_{6,\mathrm{m}}^{SH,\varepsilon_1}\left|\psi_4^{IV}\right\rangle \qquad (37)$$
$$m = 1-6,$$

where the 'girdle functions' (the ones with Roman numerals) for the SH have to be expressed in site functions analogously to the ones for the NH. But, for that the corresponding matrices ($\boldsymbol{V}^{IV-VI}$) for the SH need to be checked to see whether a reorientations step is needed for one-to-one interaction between functions of degenerate IR types (see below, next section). In the above, explicit expressions given for the $\mathcal{E}_1$ IR hold similarly for the other IRs.

In fig. 2 a schematic picture of the computational scheme is presented (for the IR $\mathcal{E}_1$, the other schemes are the similar ($\mathcal{E}_2$) or simpler ($\mathcal{A}_1$)) showing all the important steps, discussed above apart from the coupling scheme for the two hemispheres, to be discussed next.

III.6 Eigensolutions for the Bucky Ball

Next, relations will be derived to couple solutions of the NH to those of SH, the latter being basically identical to the former ones, but some reorientation of the basic functions of the doubly degenerate IRs is required in relation to the desired one-by-one interactions. The Hamiltonian describing the interaction between the two hemispheres is given by:

$$\mathcal{H}_{NS} = t\sum_{m=1}^{10}\left|m\right\rangle^{IV}\left\langle m+1 \bmod 10\right|^{III} + \text{adjoint}\,. \qquad (38)$$

We first consider $\mathcal{E}_1$ IRs; the other ones can be treated similarly or in a simpler way (the nondegenerate $\mathcal{A}_1$ states do not need a 'reorientation'). For the computation of the coupling strength between the two hemispheres one needs to know matrix $\boldsymbol{V}^{IV}$, which follows from $\boldsymbol{V}^{III}$, but a reorientation (here discussed for the $\mathcal{E}_1$ IRs) turns out to be required. For later use (in order to be able to express the eigenfunctions in terms of all site functions involved) also the matrices $\boldsymbol{V}^{V}$ and $\boldsymbol{V}^{VI}$ need a reorientation step. Focussing first on $\boldsymbol{V}^{IV}$, the reorientation should be such that the operator in eq. 38 induces interaction only as indicated by the arrows:

$$\psi_{1,3}^{III} \xleftrightarrow{\mathcal{H}_{NS}} \psi_{1,3}^{IV};\ \psi_{2,4}^{III} \xleftrightarrow{\mathcal{H}_{NS}} \psi_{2,4}^{IV}\,. \qquad (39)$$

Using the approach given in the Appendix we arrive at the following transformation for the eigenfunctions $\left|\psi_{1:4}\right\rangle^{IV}$ computed with the aid of:

$$\begin{aligned}\boldsymbol{V}_{:,m}^{IV} &= \cos\theta_1\boldsymbol{V}_{:,m}^{III} + \sin\theta_1\boldsymbol{V}_{:,m+1}^{III}\\ \boldsymbol{V}_{:,m+1}^{IV} &= -\sin\theta_1\boldsymbol{V}_{:,m}^{III} + \cos\theta_1\boldsymbol{V}_{:,m+1}^{III},\ m=1,3;\ \theta_1 = -0.2\pi\end{aligned} \qquad (40)$$

In the spirit of the group theoretical property number 10 (sect. II.2), it follows:

$$\begin{aligned}\boldsymbol{V}_{:,m}^{V} &= \cos\theta_1\boldsymbol{V}_{:,m}^{II} + \sin\theta_1\boldsymbol{V}_{:,m+1}^{II}\\ \boldsymbol{V}_{:,m+1}^{V} &= -\sin\theta_1\boldsymbol{V}_{:,m}^{II} + \cos\theta_1\boldsymbol{V}_{:,m+1}^{II},\ m=1,3,5\\ \boldsymbol{V}_{:,1}^{VI} &= \cos\theta_1\boldsymbol{V}_{:,1}^{I} + \sin\theta_1\boldsymbol{V}_{:,2}^{I}\\ \boldsymbol{V}_{:,2}^{VI} &= -\sin\theta_1\boldsymbol{V}_{:,1}^{I} + \cos\theta_1\boldsymbol{V}_{:,2}^{I}\end{aligned} \qquad (41)$$

Checking the results of computations we found indeed the desired one by one interaction.

Next, using a different value for the 'reorientation' angle, vectors of the $\mathcal{E}_2$ IRs, being $\boldsymbol{V}_{:,5-8}^{IV}, \boldsymbol{V}_{:,7-12}^{V}, \boldsymbol{V}_{:,3-4}^{VI}$, can be computed similarly. The required rotation angle is found to be equal to $\theta_2 = -0.4\pi$.

Now we are ready to present the interaction matrix for the $\mathcal{E}_1$ IRs for the full BB, which is given by:

$$\boldsymbol{M}^{BB}_{\mathcal{E}_1} = \begin{pmatrix} \boldsymbol{D}^{NH,\mathcal{E}_1} & \boldsymbol{G} \\ \boldsymbol{G} & \boldsymbol{D}^{NH,\mathcal{E}_1} \end{pmatrix} \begin{matrix} \left|\psi^{NH,\mathcal{E}_1,\alpha}_{1\text{–}6}\right\rangle \\ \left|\psi^{SH,\mathcal{E}_1,\alpha}_{1\text{–}6}\right\rangle \end{matrix} \quad G_{ml} = \left\langle \psi^{SH,\mathcal{E}_1,\alpha}_m \middle| \mathcal{H}_{NS} \middle| \psi^{NH,\mathcal{E}_1,\alpha}_l \right\rangle \tag{42}$$

where $\boldsymbol{D}^{NH,\mathcal{E}_1}$ is a diagonal matrix with on the diagonal the entries of $\boldsymbol{E}^{NH,\mathcal{E}_1}$, defined in eq. 33. An expansion of the functions mentioned above is given below showing only terms that matter for the entries of $\boldsymbol{G}$ accounting for the interaction between site functions of Girdle III with those of Girdle IV:

$$\begin{aligned} \left|\psi^{NH,\mathcal{E}_1,\alpha}_l\right\rangle &= V^{NH,\mathcal{E}_1}_{5,l}\left|\psi^{III}_1\right\rangle + V^{NH,\mathcal{E}_1}_{6,l}\left|\psi^{III}_3\right\rangle + .. = \sum\nolimits_{r=1}^{10}\left(V^{NH,\mathcal{E}_1}_{5,l}V^{III}_{r1} + V^{NH,\mathcal{E}_1}_{6,l}V^{III}_{r3}\right)\left|r\right\rangle^{III} + .. \\ \left|\psi^{SH,\mathcal{E}_1,\alpha}_m\right\rangle &= V^{NH,\mathcal{E}_1}_{5,m}\left|\psi^{IV}_1\right\rangle + V^{NH,\mathcal{E}_1}_{6,m}\left|\psi^{IV}_3\right\rangle + .. = \sum\nolimits_{r=1}^{10}\left(V^{NH,\mathcal{E}_1}_{5,m}V^{IV}_{r1} + V^{NH,\mathcal{E}_1}_{6,m}V^{IV}_{r3}\right)\left|r\right\rangle^{IV} + .. \end{aligned} \tag{43}$$

From the nature of considered Hamiltonian (see eq. 38) it follows that the sub-matrix $\boldsymbol{G}$ is symmetric. Once the eigenvectors and eigenvalues of the above (also symmetric) matrix $\boldsymbol{M}$ have been solved the results, which hold for both the α and β functions of the $\mathcal{E}_1$ IRs, can be used for further computations.

Similarly, expressions for the $\mathcal{E}_2$ and $\mathcal{A}_1$ IRs can be derived, leading to (together with results above) the eigenvectors (columns of the $\boldsymbol{V}$ matrices) and eigenvalues, which are denoted by

$$\boldsymbol{V}^{BB,\mathcal{E}_1}, \boldsymbol{V}^{BB,\mathcal{E}_2}, \boldsymbol{V}^{BB,\mathcal{A}_1} \text{ and } \boldsymbol{E}^{BB,\mathcal{E}_1}, \boldsymbol{E}^{BB,\mathcal{E}_2}, \boldsymbol{E}^{BB,\mathcal{A}_1}, \tag{44}$$

being matrices and vectors, respectively, of order 12. For completeness we give below an example of an expression for the eigenfunctions of the full BB, for functions of the β type with $\mathcal{E}_2$ symmetry, to which the entries of the above $\boldsymbol{V}$-matrices apply:

$$\left|\psi^{BB,\mathcal{E}_2,\beta}_m\right\rangle = \sum\nolimits_{l=1}^{6}\left(V^{BB,\mathcal{E}_2}_{l,m}\left|\psi^{NH,\mathcal{E}_2,\beta}_l\right\rangle + V^{BB,\mathcal{E}_2}_{l+6,m}\left|\psi^{SH,\mathcal{E}_2,\beta}_l\right\rangle\right),\ m = 1\!:\!12\,. \tag{45}$$

III.7 Eigenfunctions of the full BB expressed in site functions

The expressions for the above BB eigenfunctions in terms of the site functions of the girdles I-III (NH) can be found above (sect. II.1-4). Those for the SH are identical, apart from the fact that these refer to different girdles and the 'reorientation' transformations given by eqs. 40 and 41.

As an example we will next write out the eigenfunctions given in eq. 45 of the β type with $\mathcal{E}_2$ symmetry:

$$\begin{aligned} &\left|\psi^{BB,\mathcal{E}_2,\beta}_m\right\rangle = \sum\nolimits_{l=1}^{6}\left(V^{BB,\mathcal{E}_2}_{l,m}\left|\psi^{NH,\mathcal{E}_2,\beta}_l\right\rangle + V^{BB,\mathcal{E}_2}_{l+6,m}\left|\psi^{SH,\mathcal{E}_2,\beta}_l\right\rangle\right),\ m = 1\!:\!12,\ \text{with:} \\ &\text{with}\ \left|\psi^{NH,\mathcal{E}_2,\beta}_l\right\rangle = V^{NH,\mathcal{E}_2}_{1,l}\left|\psi^{I}_4\right\rangle + V^{NH,\mathcal{E}_2}_{2,l}\left|\psi^{II}_8\right\rangle + V^{NH,\mathcal{E}_2}_{3,l}\left|\psi^{II}_{10}\right\rangle + \\ &\qquad V^{NH,\mathcal{E}_2}_{4,l}\left|\psi^{II}_{12}\right\rangle + V^{NH,\mathcal{E}_2}_{5,l}\left|\psi^{III}_6\right\rangle + V^{NH,\mathcal{E}_2}_{6,l}\left|\psi^{III}_8\right\rangle \\ &\text{and}\ \left|\psi^{SH,\mathcal{E}_2,\beta}_l\right\rangle = V^{NH,\mathcal{E}_2}_{1,l}\left|\psi^{VI}_4\right\rangle + V^{NH,\mathcal{E}_2}_{2,l}\left|\psi^{V}_8\right\rangle + V^{NH,\mathcal{E}_2}_{3,l}\left|\psi^{V}_{10}\right\rangle + \\ &\qquad V^{NH,\mathcal{E}_2}_{4,l}\left|\psi^{V}_{12}\right\rangle + V^{NH,\mathcal{E}_2}_{5,l}\left|\psi^{IV}_6\right\rangle + V^{NH,\mathcal{E}_2}_{6,l}\left|\psi^{IV}_8\right\rangle \end{aligned} \tag{46}$$

Further decomposition in terms of site functions is rather straight forward and can be accomplished with eq. 11 and the explanation leading to eqs. 25, 28, 40 and 41.

To simplify the notation we rewrite the 60 eigenfunctions of BB as follows:

$$\left|\psi^{BB,\mathcal{E}_1,\alpha}_{1:12}\right\rangle, \left|\psi^{BB,\mathcal{E}_1,\beta}_{1:12}\right\rangle, \left|\psi^{BB,\mathcal{E}_2,\alpha}_{1:12}\right\rangle, \left|\psi^{BB,\mathcal{E}_2,\beta}_{1:12}\right\rangle, \left|\psi^{BB,\mathcal{A}_1}_{1:12}\right\rangle \xrightarrow{\text{rewrite}} \left|\phi^{BB}_s\right\rangle,\ s = 1\!:\!60, \tag{47}$$

where the ordering may be arbitrary. For some applications however (as presented below, see eq. 57) the states can most conveniently ordered per energy level, with degenerate states grouped together. For such a reordering one might choose e.g. an ascending order.

III.8 Eigenvalues and a few notes on evaluating the NoWs

The energy levels of the 60 eigenstates of the BB are graphically presented in fig. 3 by horizontal lines; also the corresponding – ordered according to their values - energy levels $E_{1:60}$ are indicated. The density of states (DoS) are presented using convolution)of the delta functions representing a single state) with a Gaussian function with weight equal to unity and a $1/e$ full width of $w = 0.2$ ($t = 1$). The integrated DoS leads to integral values of 24, 24, 12 for the three IRs (which add up to 60 as it should). The degeneracies can be inferred from the subscripts to 'E', near the lines indicating the energy values, and also from the corresponding peak height: a stand-alone peak corresponding to a singlet has a peak height of 5.64 ($= 2/(w\sqrt{\pi})$).

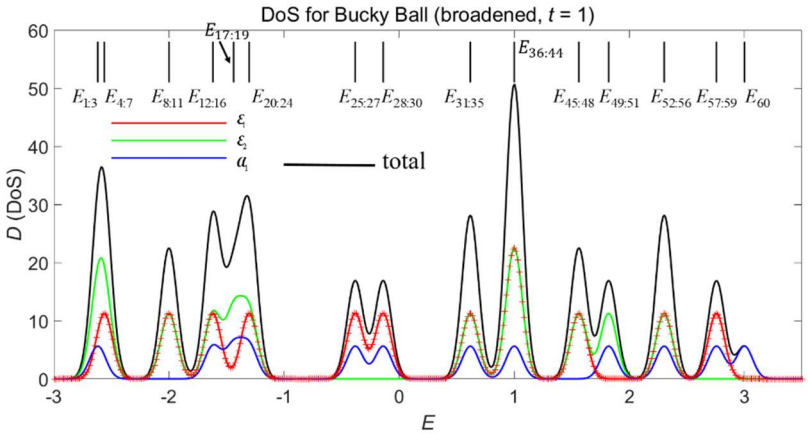

Figure 3. *The computed DoS of the full BB. The curves represent the DoS, split out according to the IRs and the sum of these (black). The vertical lines indicate the energy values of the eigenstates; the subscripts to E represents the numbering of the states.*

It is seen that a relatively large number of these have an eigenvalue of 1 (with an inaccuracy of ~1e-15 in its computed values); here and below we will use units of t for energy values. It is also noted that many eigenvalues correspond to relatively simple expressions as $(1+\sqrt{13})/2 \sim 2.3028$ and $(\sqrt{5}-1)/2 \sim 0.6180$ and $(-\sqrt{5}-1)/2 \sim -1.6180$ which seems to suggest that there may exist a more analytical approach to considered eigenvalue problem. It is found that there are fifteen different energy levels, where small differences (attributed to numerical inaccuracies) between two nearby lying levels are neglected. The largest eigenvalue is $\left(E_{12}^{BB,a_1} = \right) 3$, which corresponds to a state to which all site functions contribute equally (and which is for that reason an a_1 state) with eigenfunction

$$\left|\psi_{12}^{BB,a_1}\right\rangle = \frac{1}{\sqrt{60}} \sum_{\text{all sites}} \left|m\right\rangle, \tag{48}$$

as can be proved easily by applying the Hamiltonian $\mathcal{H}$ to the function at the rhs of eq. 48. It is found that this state has the largest energy, also in absolute sense, as it should according to a simple argument given below eq. 50.

With the NoW eq. and the notation of the previous section for the eigenfunctions (eq. 47) we arrive at the following expression for the NoWs:

$$W_{l,m}^{(M)} = \sum_{s=1}^{60}\left[\left(E_s^{BB}\right)^M \left\langle l\middle|\phi_s^{BB}\right\rangle\left\langle\phi_s^{BB}\middle|m\right\rangle\right] \equiv \sum_{s=1}^{60}\left[\left(E_s^{BB}\right)^M U_s^{(lm)}\right];\quad U_s^{(lm)} \equiv \left\langle l\middle|\phi_s^{BB}\right\rangle\left\langle\phi_s^{BB}\middle|m\right\rangle \tag{49}$$

where $|l\rangle$ and $|m\rangle$ can be chosen arbitrarily out of the 60 site functions. It is seen that for large M the dominant contribution to the NoWs comes from the a_1 state with eigenvalue 3. Then, it follows, also using

$$U_{60}^{(lm)}\left(\equiv \left\langle l\middle|\psi_{12}^{BB,a_1}\right\rangle\left\langle\psi_{12}^{BB,a_1}\middle|m\right\rangle\right) = 1/60,\ \forall l,m \text{ as: } \left|\psi_{12}^{BB,a_1}\right\rangle = \left|\phi_{60}^{BB}\right\rangle, \tag{50}$$

(which is seen with eqs. 48-49) that the asymptotic behaviour of the NoWs should be:

$$W_{l,m}^{(M)} \propto 3^M/60,\ \text{if } M\to\infty,\ \forall l,m. \tag{51}$$

Considering eq. 49 one may deduce that the largest absolute value of the eigenvalues should correspond to a positive eigenvalue: otherwise the NoWs will become negative for large odd values of M. It is further seen from eq. 49 that all information on the considered sites (l,m) as used in the computation of W is contained in the vector of length 60, U.

For the evaluation of expressions like eq. 49 careful bookkeeping is required using the expressions of previous section; a few examples of written out inner products needed for that are given below (where we used the original notation for identification of the eigenfunctions):

$$\begin{aligned}
&{}^{I}\left\langle P\middle|\psi_m^{BB,\varepsilon_1,\alpha}\right\rangle = \sum_{l=1}^{6}\left(V_{l,m}^{BB,\varepsilon_1}V_{1,l}^{NH,\varepsilon_1}V_{P,1}^{I}\right);\ {}^{I}\left\langle P\middle|\psi_m^{BB,\varepsilon_1,\beta}\right\rangle = \sum_{l=1}^{6}\left(V_{l,m}^{BB,\varepsilon_1}V_{1,l}^{NH,\varepsilon_1}V_{P,2}^{I}\right)\\
&{}^{II}\left\langle P\middle|\psi_m^{BB,\varepsilon_1,\alpha}\right\rangle = \sum_{l=1}^{6}\left\{V_{l,m}^{BB,\varepsilon_1}\left(V_{2,l}^{NH,\varepsilon_1}V_{P,1}^{II}+V_{3,l}^{NH,\varepsilon_1}V_{P,3}^{II}+V_{4,l}^{NH,\varepsilon_1}V_{P,5}^{II}\right)\right\}\\
&{}^{II}\left\langle P\middle|\psi_m^{BB,\varepsilon_1,\beta}\right\rangle = \sum_{l=1}^{6}\left\{V_{l,m}^{BB,\varepsilon_1}\left(V_{2,l}^{NH,\varepsilon_1}V_{P,2}^{II}+V_{3,l}^{NH,\varepsilon_1}V_{P,4}^{II}+V_{4,l}^{NH,\varepsilon_1}V_{P,6}^{II}\right)\right\}\\
&{}^{II}\left\langle P\middle|\psi_m^{BB,\varepsilon_2,\alpha}\right\rangle = \sum_{l=1}^{6}\left\{V_{l,m}^{BB,\varepsilon_2}\left(V_{2,l}^{NH,\varepsilon_2}V_{P,7}^{II}+V_{3,l}^{NH,\varepsilon_2}V_{P,9}^{II}+V_{4,l}^{NH,\varepsilon_2}V_{P,11}^{II}\right)\right\}\\
&{}^{IV}\left\langle P\middle|\psi_m^{BB,\varepsilon_1,\alpha}\right\rangle = \sum_{l=1}^{6}\left\{V_{l+6,m}^{BB,\varepsilon_1}\left(V_{5,l}^{NH,\varepsilon_1}V_{P,1}^{IV}+V_{6,l}^{NH,\varepsilon_1}V_{P,3}^{IV}\right)\right\},\ P\text{: site number}
\end{aligned} \tag{52}$$

In the above P is the site number of the girdle indicated by the Roman super script, and the matrices $\boldsymbol{V}$ where introduced in sect^s. II and III.1-7. It is seen that some bookkeeping is required to arrive at the above equations, but basically it straightforward and follows by consulting carefully the relations in sect. III.1-7.

For numerical evaluation of the NoWs and also of the number of visits – introduced below – it is computationally efficient to re-order the eigensolutions according to their energies, in order to exploit their relatively large degeneracy. The reordering used by us is depicted in fig. 3 with degeneracies, $N_{D,1:15}$, for the 15 levels, denoted by $E_{1:15}^L$, given by:

$$N_{D,1:15} = (3\,4\,4\,5\,3\,5\,3\,3\,5\,9\,4\,3\,5\,3\,1). \tag{53}$$

With the above re-ordering one may rewrite eq. 49 into a bit simpler fashion which may speed up computations:

$$W_{l,m}^{(M)} = \sum_{r=1}^{15}\left[\left(E_r^L\right)^M \sigma_r^{(l,m)}\right],\ \sigma_r^{(l,m)} \equiv \sum_{s=P_r+1}^{P_r+N_r} U_s^{(lm)},\ P_{r(\geq 2)} \equiv \sum_{p=1}^{r-1} N_{D,r},\ P_1 = 0. \tag{54}$$

The quantities $60\sigma_{1:15}^{(l,m)}$ are presented in fig. 4 as a function of $E_{1:15}^L$; note that the quantity $\sigma_n^{(l,m)}$ corresponds to the n^{th} level. The factor 60 was used to show that the values of $60\sigma_{1:15}^{(l,m)}$ for the case $l = m$ (black line in the figure) represent the degeneracies of the levels involved, as follows from

symmetry arguments. So, as is seen now quite clearly from eq. 54: the NoWs to travel from (arbitrarily chosen) site l to site m on the BB in M steps is computed (only) from two series of both 15 entries. And all the computed NoWs are (of course) whole numbers (ideally) which should indicate a special relation between the 30 real numbers involved (which is not investigated here).

Considering fig. 4 it is seen that, if $l = m$, the numbers $\sigma_{1:15}^{(l,l)}$ (representing, apart from a factor 60, the degeneracies of the levels, as noted above) are all positive. The other series $\sigma_{1:15}^{(l,m)}$, $l \neq m$ show considerably more variation as a function of $E_{1:15}^{L}$, an effect which seems to increase with the distance on the BB between the two sites involved (as we found also considering results not presented here). The case $(l,m) = (|1\rangle^{I}, |5\rangle^{VI})$ is quite special: the two sites are at maximum distance which apparently – as we found – leads to the following

$$\sigma_{1:15}^{(p,p)} = \left|\sigma_{1:15}^{(l,m)}\right|,\ l = |1\rangle^{I},\ m = |5\rangle^{VI},\ \forall p, \tag{55}$$

a property which we attribute to the symmetry of the considered situation; we did not investigate this further.

The strong oscillatory (from positive to negative values!) behaviour of $\sigma_{1:15}^{(l,m)}$ for l and m being far (say, 5 or 6 steps) apart can be understood (a bit) in the light of eq. 54 (showing the presence of rapidly varying contributions of the energy terms, M if it changes from odd to even and vice versa) and the fact that the NoWs should be all zero for 5 or 6 separating steps.

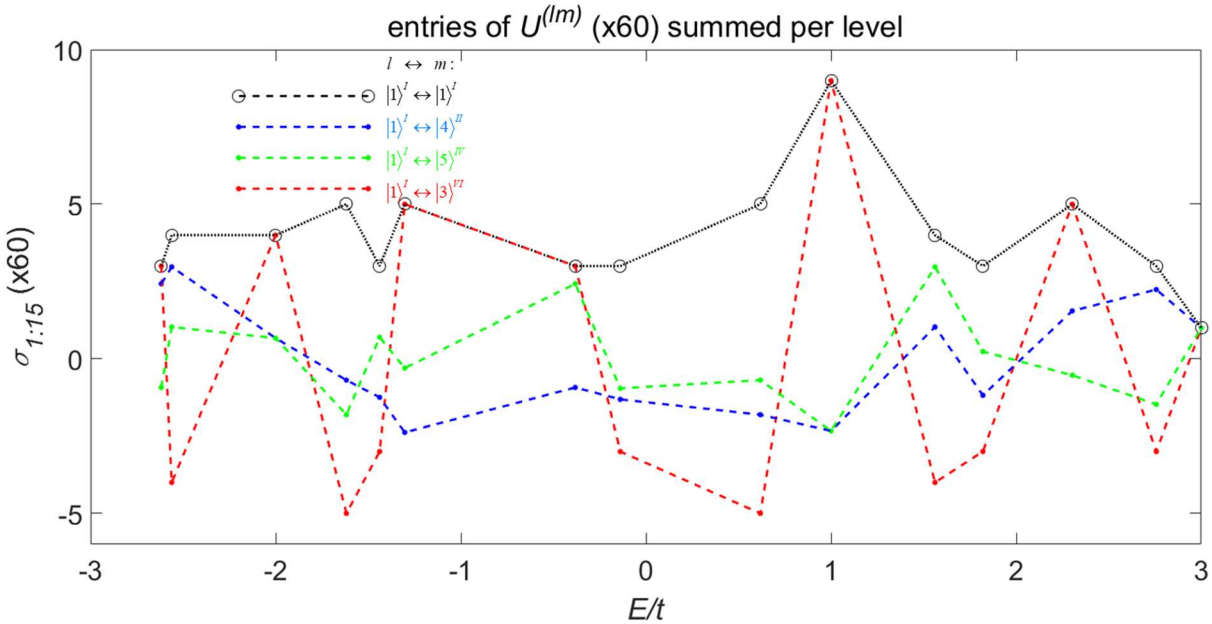

Figure 4. *The quantities* $\sigma_{1:15}^{(l,m)}$ *– defined by eq.* 54 *– as a function of* $E_{1:15}^{L}$*, with (l,m) according to the inset text; the dashed and dotted lines serve as a guide to the eyes. The results for* $(l,m) = (|1\rangle^{I}, |1\rangle^{I})$ *also represent the degeneracy of the corresponding levels (see text above).*

III.9 Travelling via specified intermediate sites: The number of visits.

As discussed in this section: The above approach enables the use of analytical expressions to evaluate for example the number of visits (NoVs) to a certain intermediate site while stepping –with M steps – from site l to site m. Also visits to a certain combination of sites, possibly also specifying the number or allowed range of intermediate steps, can be expressed in analytical

form with the formalism. For the NoVs we will use the symbol V with the superscript denoting the total number of steps (M) and the subscripts denoting constraints on considered trajectories. In this section a number of examples to the above, with corresponding expressions, will be presented. A first example is

$$V^{(M)}_{l\{L\}p\{M-L\}m}, \text{ with e.g. } L=1:M-1 \text{ or } L=4:M-3 \ (M\geq 7) \tag{56}$$

where sites l and m are the starting and end points of each considered trip – with M steps –; the intermediate site is denoted by p and the numbers between brackets {} present the considered number or range of steps between sites given adjacent to these brackets (i.e., between sites l and p and between sites p and m). The NoVs to site p, taking into account all possible NoWs to travel from site l to site m in M steps, can be evaluated with the following expression constructed in the same spirit as eq. 49:

$$V^{(M)}_{l\{L\}p\{M-L\}m}=\sum_{L=1}^{M-1}\left(\sum_{s=1}^{60}\left[\left(E_s^{BB}\right)^{M-L}U_s^{(lp)}\right]\sum_{\sigma=1}^{60}\left[\left(E_\sigma^{BB}\right)^{L}U_\sigma^{(pm)}\right]\right),\ L=1:M-1, \tag{57}$$

where in the summation with L running from 1 to M-1 the number of steps between sites l and p are varied, such that the total number of steps is always M. Note that in the above the summation is such (via $1\leq L\leq M-1$) that in considered trajectories there is at least one step between sites p and l and between sites p and m (which does not exclude that for example p = m). The above can be rewritten as:

$$\begin{aligned}
&V^{(M)}_{l(L=1:M-1)p(M-L)m}=\boldsymbol{a}^t\boldsymbol{Z}^{(M)}\boldsymbol{b}\\
&\text{with}\\
&a_s\equiv U_s^{(lp)},\ b_\sigma\equiv U_\sigma^{(pm)},\ s,\sigma=1,..,60\\
&\quad Z^{(M)}_{s\sigma}\equiv\sum_{L=1}^{M-1}\left(E_s^{BB}\right)^{M-L}\left(E_\sigma^{BB}\right)^{L}=\\
&E_s^{BB}\neq E_\sigma^{BB}:\ A\frac{1-r^{M-1}}{1-r}=E_s^{BB}E_\sigma^{BB}\frac{\left(E_s^{BB}\right)^{M-1}-\left(E_\sigma^{BB}\right)^{M-1}}{E_s^{BB}-E_\sigma^{BB}};\begin{cases}A\equiv\left(E_s^{BB}\right)^{M-1}E_\sigma^{BB}\\ r\equiv E_\sigma^{BB}/E_s^{BB}\end{cases}\\
&E_s^{BB}=E_\sigma^{BB}:\ \ Z^{(M)}_{ss}=\sum_{N=1}^{M-1}\left(E_s^{BB}\right)^{M}=(M-1)\left(E_s^{BB}\right)^{M}
\end{aligned} \tag{58}$$

where the symbols U where introduced in eq. 49 and it is seen that $\boldsymbol{a}$ and $\boldsymbol{b}$ are vectors of length 60 and $\boldsymbol{Z}$ is a 60x60 symmetric matrix, which can all straightforwardly be evaluated with presented theory. It is seen from eq. 58 that the NoVs can be expressed as a product of terms involving the overlap between site functions and eigenfunctions and a matrix with entries depending on the state energies. Owing to the large degeneracies occurring in the solutions a large number of these entries are identical which opens a way to reduce the evaluation time.
With a similar reasoning as used to find eq. 51 it can be found that the asymptotic behaviour of considered NoVs is given by:

$$V^{(M)}_{l(L=1:M-1)p(M-L)m}\propto(M-1)\left(E_{15}^{L}\right)^{M}/60^2,\ \text{if } M\to\infty,\ \forall l,m,p;\ E_{15}^{L}=3. \tag{59}$$

The factor $M-1$ in the above shows that – for considered large values of M – the NoVs exceed by far the corresponding NoWs (see also eq. 51). The latter is related to the fact that there may be – for large M values – a large number of visits to the intermediate site p within one of the ways contributing to the NoWs.
As an extension to the above we next consider expressions for the number of pair visits to travel between sites l to site m in M steps, with two sites, say, p and q, being intermediate sites and being visited in given order, which can be expressed as – arguing in a similar way as above:

$$V^{(M)}_{l\{P=1:M-2\}p\{Q=1:M-P-1\}q\{M-P-Q\}m} =$$

$$\sum_{P=1}^{M-2}\sum_{Q=1}^{M-P-1}\left(\sum_{s,\sigma,u=1}^{60}\left[\left(E_s^{BB}\right)^P U_s^{(lp)}\left(E_\sigma^{BB}\right)^Q U_\sigma^{(pq)}\left(E_u^{BB}\right)^{M-P-Q} U_u^{(qm)}\right]\right)\equiv$$

$$\sum_{P=1}^{M-2}\sum_{Q=1}^{M-P-1}\left(\sum_{s,\sigma,u=1}^{60}\left[\Phi_{s,\sigma,u}\Gamma^{M,P,Q}_{s,\sigma,u}\right]\right)\equiv\sum_{s,\sigma,u=1}^{60}\left[\Phi_{s,\sigma,u}\Psi_{s,\sigma,u}\right], \qquad (60)$$

with $\Phi_{s,\sigma,u}\equiv U_s^{(lp)}U_\sigma^{(pq)}U_u^{(qm)}$; $\Psi_{s,\sigma,u}\equiv\sum_{P=1}^{M-2}\sum_{Q=1}^{M-P-1}\Gamma^{M,P,Q}_{s,\sigma,u}$

and $\Gamma^{M,P,Q}_{s,\sigma,u}\equiv\left(E_s^{BB}\right)^P\left(E_\sigma^{BB}\right)^Q\left(E_u^{BB}\right)^{M-P-Q}$.

In the above it was assumed that there is at least one step between sites p and q as well as between the pairs (l,p) and (q,m). The summations for the evaluation of Ψ can be simplified to:

if $E_s^{BB}\neq E_\sigma^{BB}\neq E_u^{BB}\neq E_s^{BB}$:

$$\Psi_{s,\sigma,u}=\sum_{P=1}^{M-2}\left(E_s^{BB}\right)^P E_\sigma^{BB}E_u^{BB}\frac{\left(E_u^{BB}\right)^{M-P-1}-\left(E_\sigma^{BB}\right)^{M-P-1}}{E_u^{BB}-E_\sigma^{BB}}=E_s^{BB}E_\sigma^{BB}E_u^{BB}\cdot$$

$$\frac{E_\sigma^{BB}\left(\left(E_u^{BB}\right)^{M-1}-\left(E_s^{BB}\right)^{M-1}\right)-E_s^{BB}\left(\left(E_u^{BB}\right)^{M-1}-\left(E_\sigma^{BB}\right)^{M-1}\right)+E_u^{BB}\left(\left(E_s^{BB}\right)^{M-1}-\left(E_\sigma^{BB}\right)^{M-1}\right)}{\left(E_u^{BB}-E_\sigma^{BB}\right)\left(E_u^{BB}-E_s^{BB}\right)\left(E_\sigma^{BB}-E_s^{BB}\right)}$$

if $E_\sigma^{BB}=E_u^{BB}\neq E_s^{BB}$: (61)

$$\Psi_{s,\sigma,\sigma}=\sum_{P=1}^{M-2}\sum_{Q=1}^{M-P-1}\left(\left(E_s^{BB}\right)^P\left(E_\sigma^{BB}\right)^{M-P}\right)=$$

$$=\frac{-(M-1)\left(E_s^{BB}\right)^2\left(E_\sigma^{BB}\right)^M+\left(E_s^{BB}\right)^M\left(E_\sigma^{BB}\right)^2+(M-2)E_s^{BB}\left(E_\sigma^{BB}\right)^{M+1}}{\left(E_\sigma^{BB}-E_s^{BB}\right)^2}$$

if $E_s^{BB}=E_\sigma^{BB}=E_u^{BB}$:

$$\Psi_{s,s,s}=\sum_{P=1}^{M-2}\sum_{Q=1}^{M-P-1}\left(E_s^{BB}\right)^M=0.5\left(M^2-3M+2\right)\left(E_s^{BB}\right)^M.$$

For the evaluation of $V^{(M)}_{l\{P=1:M-2\}p\{Q=1:M-P-1\}q\{M-P-Q\}m}$ it could save computation time to use that there are only ($S=$) 15 different energy levels; these lead to 680 different combinations of terms with three energies and so to as many different values of $\Psi_{s,\sigma,u}$. These 680 (=455 + 210 +15) different combinations result from

$$\binom{S}{3}=455 \text{ (3 different } E's),\ S(S-1)=210 \text{ (2 identical } E's),\ 15 \text{ (3 indetical } E's),$$

with S=60 the number of states. With states ordered to their energies advantage can be taken from the relatively large degeneracy: instead of 60^3 evaluations of products involving three energy values only 680 evaluations are needed.

It is left as an exercise for the reader to that prove the following expression holds:

$$V^{(M)}_{l\{P=1:M-2\}p\{Q=1:M-P-1\}q\{M-P-Q\}m}\propto 0.5(M^2-3M+2)3^M/60^3,\ \textit{if}\ M\to\infty,\ \forall l,m,p,q. \qquad (62)$$

IV. Computational results and discussion

In this section a few results of NoWs and NoVs computations – illustrating the above theory – will be presented and discussed.

IV.1 A note on the computational accuracy

At first the NoWs eq. 49 will be considered. One may expect that the results obtained with it are integers, apart from numerical differences related to the inaccuracy of the computations. We found however – with straightforward application of eq. 49 – deviations of typically $\delta \sim 10^{-2}$ which is far more than expected. It was noted that while (only) varying the number of steps M this deviation δ remained *constant* (suggesting a role of states with energy equal to unity ($t = 1$) as this value is independent of the power M; see also eq. 49). It was found that the error (caused by an error in the software, as one may assume) is originating from the computation of the matrices $\boldsymbol{V}$ introduced in eq. 44 (with rows being not exactly orthonormal). The latter leads to small errors in the quantities U defined in eq. 49. The above constancy gave the clue to repair things as follows. The error can be expressed as give below:

$$\sum_{s=1}^{60} U_s^{(lm)} = \begin{cases} \delta \ (l \neq m) \\ 1+\delta \ (l = m) \end{cases} \tag{63}$$

i.e., the quantities U deviate from the expected values (either 0 or 1). And, the errors seem to originate from functions corresponding to unit energy: $E_s = 1$. So, it is sufficient to correct one or more of the corresponding U values as in equations for both the NoWs and the NoVs the quantities E_s and $U_s^{(lm)}$ occur in pairs. To repair things in presented computations we applied:

$$\tilde{U}_s^{(lm)} = U_s^{(lm)} - \delta, \text{ one } s \text{ with } E_s = 1 \text{ (units } t), \tag{64}$$

where the tilde indicates the corrected value and s was chosen arbitrarily among the states with energy equal to inity. Doing so the *relative* deviation of the NoWs is found to be typically $\sim 10^{-14}$. For example (see also above in the text related to fig.4), our computations lead to $60\sigma_{10}^{(l,m)} = 9 + \Delta$ for both $(l,m) = (|1\rangle^I, |1\rangle^I)$ and $(l,m) = (|1\rangle^I, |5\rangle^{IV})$ with numerical errors as low as $|\Delta| \lesssim 10^{-14}$.

IV.2 NoWs computations: a few results

In this subsection results of a number of NoWs computations will be shown to give an impression of the outcomes and to show that presented approach really works and also to consider the main features of such results. Figure 5A shows computational results for stepping from site $|1\rangle^I$ to five sites in the IV^{th} girdle (see also fig. 1) in $M = 1{:}6$ steps; results for the other five sites of the IV^{th} girdle can be deduced from these, for symmetry reasons. It is seen that – also considering the site numbering in fig. 1 – computed results are in agreement with what one could expect. Such a check is no longer (easily) possible if M is increased, like for the results given in fig. 5B. Note that – for practical reasons – to get plot-data in a relatively small range – all NoWs values are multiplied with a factor $60/3^M$; having as a consequence that a decrease of the NoWs, if M goes up by 1, implies that the increase (neglecting the rare case that there is a decrease) is less than 3 (and does not mean that the NoWs goes down). In fig. 5B the strong variations of the NoWs versus M for trajectories ending at the sites numbered 1 and 2 of the IV^{th} girdle stand out; in particular if compared to results for trajectories ending at site 5 of the IV^{th} girdle. Such strong variations in the NoWs can – at least partly – be understood by taking into account the symmetry of the situation for the direct (i.e., shortest) trajectory between the pair $(|1\rangle^I, |1\rangle^{IV})$ for which $M = 3$. If M is increased to the value 5, extra new trajectories come into play owing to among other things trips along the opposite site of pentagons and hexagons; the extra increase comes (partly) from the symmetry. Intuitively one may guess that such a phenomenon does not occur to such an extent for the pair $(|1\rangle^I, |5\rangle^{IV})$ (of which the trajectories don't have above symmetry).

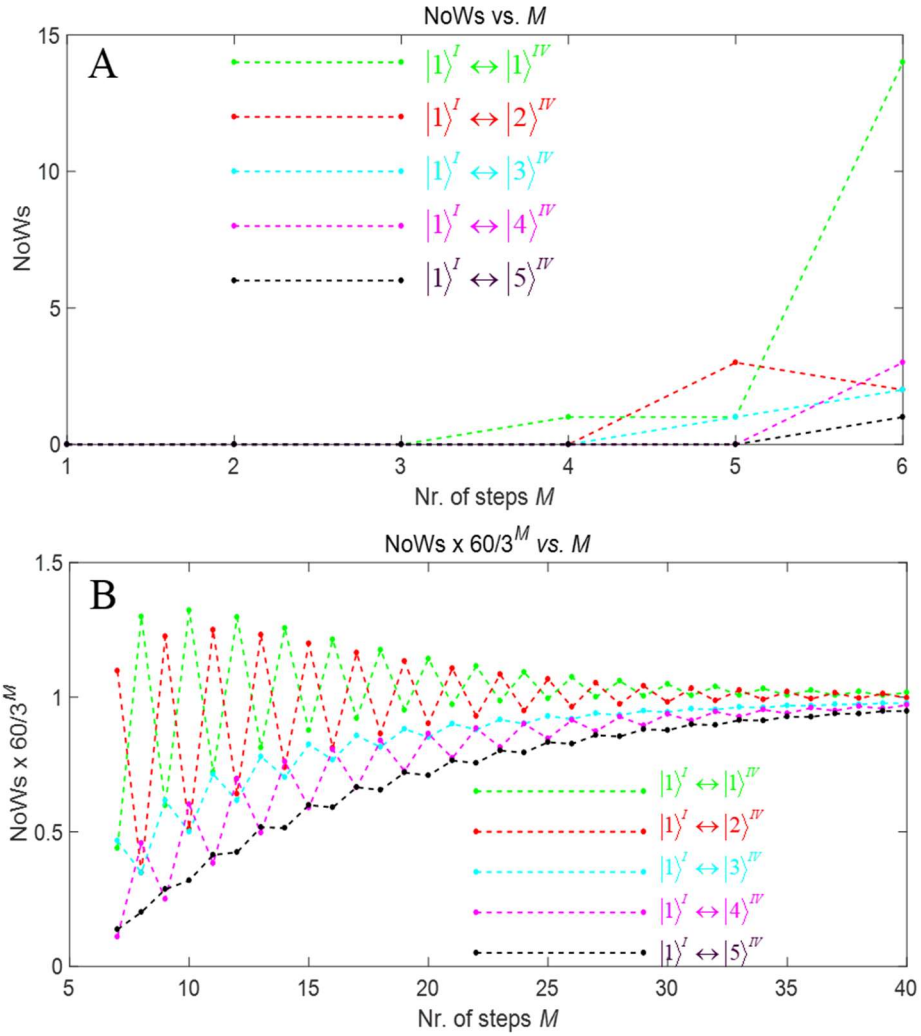

Figure 5. *(see also fig. 1), with M=1:6 steps (fig. 5A) and with M=7:40 (fig 5B). The (coloured) dots represent the results, the dashed lines are guides to the eyes.*

For the interested reader a few more results of NoWs computations – on trips between the I^{st} and VI^{th} girdles – are presented in fig. 6. The reader is encouraged to compare these with results depicted in fig. 5, and to think about the differences.

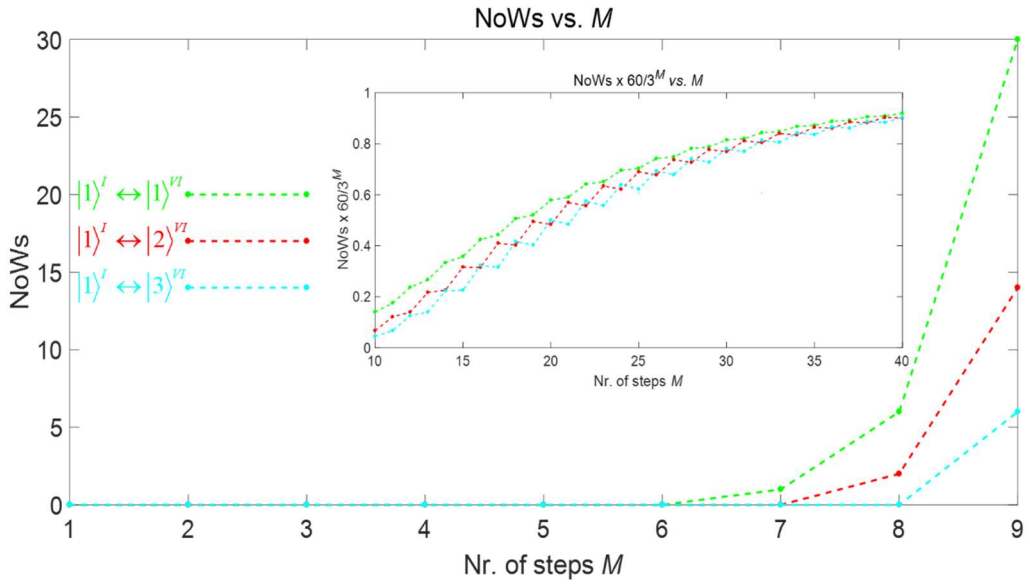

Figure 6. Computed NoWs for stepping from site $|1\rangle^I$ to sites in the VI^{th} girdle (coloured) dots with M=1:9 (main graph) and M=10:40 (inset). The dots represent the results, the dashed lines are guides to the eyes.

IV.3 NoVs computations: a few results

NoVs computations with one intermediate state

In this subsection a few results of NoVs computation will be presented, all with finish and start at neighbouring sites, being $l = |2\rangle^I$ and $m = |4\rangle^{II}$, respectively (see fig. 1) and intermediate sites, p, in the VI^{th} girdle – far removed from l and m – and also (finally) in a nearby site, $p = |4\rangle^{III}$. There are no restrictions imposed on the number of steps in between both l and p and in between p and m; the results are presented for a given total number of steps, M. Considering first the results in the main graphs of fig. 7 for $M \leq 20$ (zero values of the NoVs are not displayed) it is found that NoVs values, V, are far below those for the asymptotic limit (according to eq. 59) which is also seen in the inset of fig. 7. Such a slow start was more or less expected taking into account the (relatively) large distance between intermediate site and start and finish sites. The quantity V for $M \leq 20$ behaves approximately as being proportional to $\sim 6^M$. The considerable difference of the latter with the asymptotic value (eq. 59) can be understood by studying the entries of matrix $\boldsymbol{Z}$ in eq. 58 of which the off-diagonal elements of the 15th column and row (i.e., the 15th state –having the highest energy value in absolute sense – becomes dominant for NoVs at large M) are still considerable for M~20. This effect may cause the relatively slow convergence. But the values of the vectors U occurring in eq. 58 cause – in considered cases – that the asymptotic value is reached, from *below* (see inset of fig. 7), which is attributed to the relatively large distances between site p and both sites l and m, which will be made plausible by also considering a situation with all considered sites in close proximity (see text and fig. 8 below).

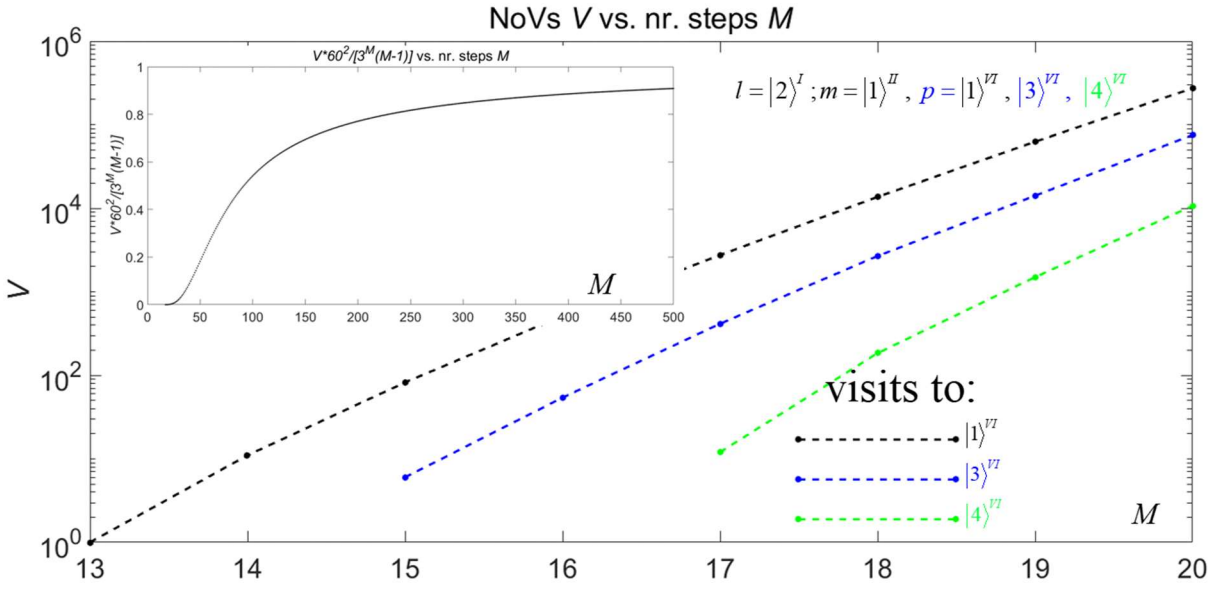

Figure 7. *Computed NoVs to indicated intermediate sites in the VIth girdle (see also fig. 1) for trajectories with start and finish being* $l = |2\rangle^{I}$ and $m = |4\rangle^{II}$ *as a function of the number of steps M, in the range M* $\leq$ *20. Zero values for the NoVs are not depicted. The results for considered case (with p far away from l and m) converge only slowly to the asymptotic value for large M (see eq.* 59) *as here demonstrated in the inset assuming* $p = |1\rangle^{VI}$.

The situation considered for fig. 8 is as for fig. 7 except for the intermediate state which is here $p = |4\rangle^{III}$, situated close to the sites *l* and *m*. It is seen in the figure that in this case the MoVs approach the asymptotic limit from above, as may be expected, which should be related to the properties of the involved *U* vectors (see eq. 58).

It is further seen in fig. 8 that for lower *M* values the NoVs increases relatively strongly if *M* is incremented by unity for even values of *M* if compared to that for odd *M* values. In the main picture of fig. 8 there seem to be two branches (one for odd and one for even *M* value) an effect which is there enhanced by the use of the *M* dependent factor. The effect has – as one may think – a similar background as that discussed above in the beginning of sect. IV.2.

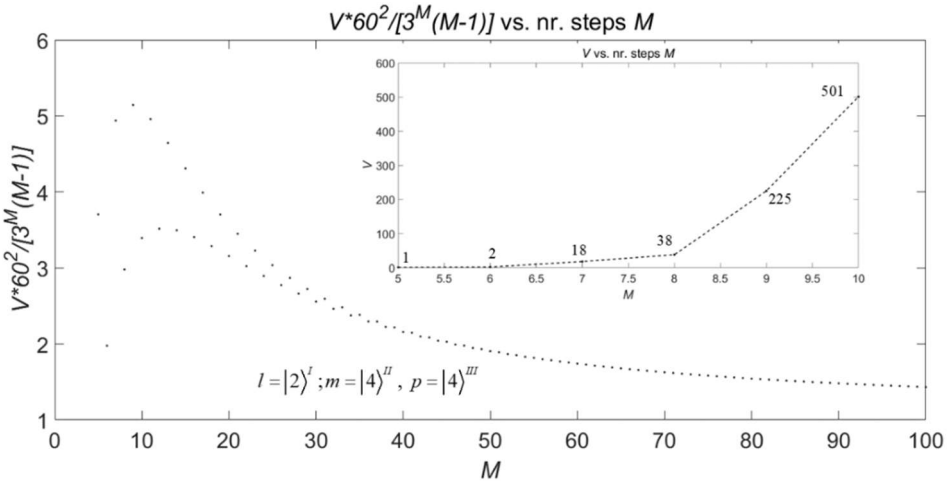

Figure 8. *Computed NoVs with visits to indicated site* $p = |4\rangle^{III}$ *and starting and end points l and m and M=5:100; the NoVs are multiplied with a factor such that the asymptotic value of V is unity for* $M \to \infty$ *(see eq.* 59*). The inset shows V for M=5:10; V=0 values (occurring for M* $\leq$ *5) are not depicted.*

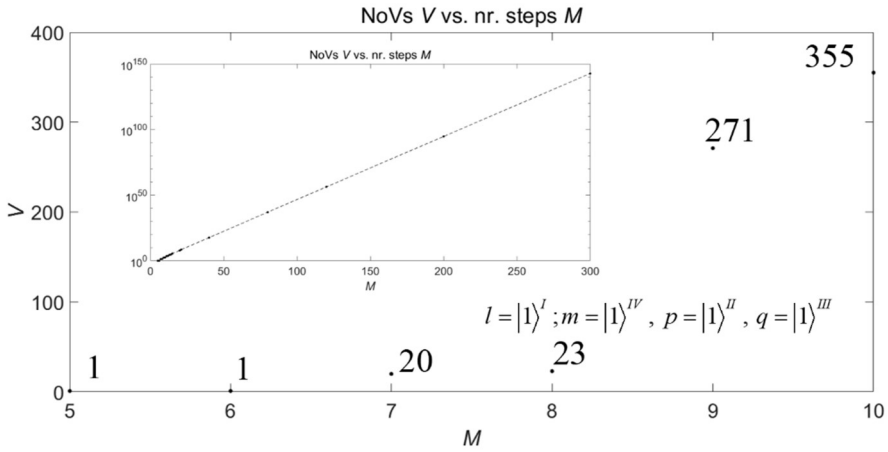

Figure 9. *Computed NoVs with visits to indicated sites* $p=|1\rangle^{II}$ *and* $q=|1\rangle^{III}$ *and with starting and end points l and m in the range M=1:10; V=0 values are not depicted. The inset concerns a semi-logarithmic plot of the same situation but the step range is much larger M=1:300. The dotted line serves as a guide to the eyes.*

NoVs computations with two intermediate states

As an illustration to eq. 61 in sect. III.9 on computations with two intermediate sites a few results will be presented and discussed in short. So, using the notation introduced earlier we will compute values of the quantity

$V^{(M)}_{l\{P=1:M-2\}p\{Q=1:M-P-1\}q\{M-P-Q\}m}$, with $l=|1\rangle^{I}$, $m=|1\rangle^{IV}$, $p=|1\rangle^{II}$, $q=|1\rangle^{III}$,

i.e., all considered sites are lying close together (see fig.1). Results are presented in fig. 9. All the computed values of V showed relative errors (computed as the *relative* difference between computed values of V and corresponding rounded of values) of around $10^{-14} - 10^{-15}$. At large M values it was found (not graphically presented here) that V is considerably larger than the corresponding asymptotic value given by eq. 62. Even at $M = 300$ the computed V is a factor two larger than the asymptotic value, which is attributed the choice of the sites involved lying all in rather close proximity.

It is further noted that the relative increase of V for increments 1 of M is much larger for even valued M if compared to odd valued M, as is seen in the figure 9. This observation can be explained in a similar way as the oscillations in fig. 5 (see text of sect IV.2), and decreases for larger M values (not shown here), as may be expected.

A *short* inspection of the outcomes of the computations of V gave us the impression that such type of computations could be helpful in the generation of prime numbers. This is seen in the above figure from the values of $V^{(8)}$ and $V^{(9)}$; and also from the values of $V^{(10)}$ (= 355) and $V^{(16)}$ (= 606014) which are multiples of prime numbers 71 and 303007, respectively, and further: $V^{(17)}$ is the product of two prime numbers 271 and 2381 as well as $V^{(17)}$ = 3x2154533 (both prime numbers).

V. A few concluding remarks

Possible application fields of presented approach have been discussed already in sect. 1.Introduction. At this point I only can ask the creative and curious reader to think about new application fields for presented theory or extensions thereof.

Appendix. Reorientation of IR function sets

Here expressions will be shown to obtain one-by-one interaction between two-fold degenerate states, using similarity transformations for part of the involved sets of basic functions. Two such sets will be considered, belonging to, say states *A* and *B* corresponding to the same IR and being eigenfunctions of symmetric (Hermitian) Hamiltonians $\mathcal{H}_A$ and $\mathcal{H}_B$, respectively. These states are interacting owing to a Hamiltonian, $\mathcal{H}_{AB}$. All here considered Hamiltonians have the symmetry of considered point group. We will choose (arbitrarily) that the functions of set *B* have to be 'reoriented'.

The interaction between the two sets *A* and *B*, via $\mathcal{H}_{AB}$, is quantified via the interaction (2-by-2) matrix $\boldsymbol{M}^{AB}$ which should generally be of the form

$$\boldsymbol{M}^{AB} \equiv \left\langle \boldsymbol{V}^A \middle| \mathcal{H}_{AB} \middle| \bar{\boldsymbol{V}}^B \right\rangle = \begin{pmatrix} M_{11}^{AB} & M_{12}^{AB} \\ M_{21}^{AB} & M_{22}^{AB} \end{pmatrix} = M^{AB} \begin{pmatrix} C & \eta S \\ -S & \eta C \end{pmatrix},\ \eta = \pm 1;\ \boldsymbol{V}^A \equiv \begin{pmatrix} \psi_1^A \\ \psi_2^A \end{pmatrix},\ \bar{\boldsymbol{V}}^B \equiv \begin{pmatrix} \bar{\psi}_1^B \\ \bar{\psi}_2^B \end{pmatrix}, \tag{65}$$

with M^{AB} a constant, $C = \cos\theta$, $S = \sin\theta$ and

$$M_{lm}^{AB} \equiv \left\langle \psi_l^A \middle| \mathcal{H}_{AB} \middle| \bar{\psi}_m^B \right\rangle,\ l,m = 1,2\,.$$

$\boldsymbol{V}^A$ and $\bar{\boldsymbol{V}}^B$ represent the orthonormal (between themselves) eigenfunctions corresponding to $\mathcal{H}_A$ and $\mathcal{H}_B$, respectively, with the bar on top indicating that the set *B* still has to be reoriented. The form of the matrix $\boldsymbol{M}^{AB}$ corresponds to the assumed symmetric Hamiltonian, where the options $\eta = \pm 1$ take into account the sign arbitrariness in choosing the signs of the functions corresponding to $\bar{\boldsymbol{V}}^B$.

The sought reorientation procedure is now simple as follows.

1. Determine η from: $\eta = \mathrm{sgn}(M_{11}^{AB} / M_{22}^{AB})$ (66)
2. The new set for the *B* solutions is:

$$\boldsymbol{V}^B \equiv \begin{pmatrix} \psi_1^B \\ \psi_2^B \end{pmatrix} = \begin{pmatrix} C & \eta S \\ -S & \eta C \end{pmatrix} \begin{pmatrix} \bar{\psi}_1^B \\ \bar{\psi}_2^B \end{pmatrix},\ \theta = \tan^{-1}\left(M_{12}^{AB} / M_{22}^{AB} \right) \tag{67}$$

With eqs. 66 and 67 one may show straightforwardly the desired one by one interaction:

$$M_{lm}^{AB} \equiv \left\langle \psi_l^A \middle| \mathcal{H}_{AB} \middle| \psi_m^B \right\rangle = \delta_{lm} M^{AB} / C;\ l,m = 1,2\,. \tag{68}$$

The above follows with $\left|\psi_1^B\right\rangle = C\left|\bar{\psi}_1^B\right\rangle + \eta S\left|\bar{\psi}_2^B\right\rangle$; $\left|\psi_2^B\right\rangle = -S\left|\bar{\psi}_1^B\right\rangle + \eta C\left|\bar{\psi}_2^B\right\rangle$:

$$\left\langle \psi_1^A \middle| \mathcal{H}_{AB} \middle| \psi_1^B \right\rangle = \left(CM_{11} + \eta S M_{12} \right) = M_{11}\left(C + \eta S M_{12} / M_{11} \right) = M_{11}(C + S^2 / C) = M_{11} / C$$

$$\left\langle \psi_1^A \middle| \mathcal{H}_{AB} \middle| \psi_2^B \right\rangle = \left(-SM_{11} + \eta C M_{12} \right) = M_{11}\left(-S + \eta C M_{12} / M_{11} \right) = 0$$

$$\left\langle \psi_2^A \middle| \mathcal{H}_{AB} \middle| \psi_1^B \right\rangle = \left(CM_{21} + \eta S M_{22} \right) = M_{22}(-\eta M_{12} / M_{22} C + \eta S) = 0$$

$$\left\langle \psi_2^A \middle| \mathcal{H}_{AB} \middle| \psi_2^B \right\rangle = \left(-SM_{21} + \eta C M_{22} \right) = M_{22}(\eta S M_{12} / M_{22} + \eta C) = \eta M_{22}(S^2 / C + C) = \eta M_{22} / C$$

References

[I] https://en.wikipedia.org/wiki/Character_table

[II] https://link.springer.com/chapter/10.1007/978-1-4612-0261-5_4 (Groups and the Buckyball Fan R. K. Chung, Bertram Kostant and Shlomo Sternberg

[III] http://symmetry.jacobs-university.de/cgi-bin/group.cgi?group=405&option=4

[IV] 4.3.3: Character Tables - Chemistry LibreTexts

[V] C.J. Ballhausen, *Introduction to Ligand Field Theory*, Mc. Graw-Hill, Book Co. Inc. (1962).